

Aluminum and Aluminum Alloys

Catrin Kammer

Part B | 6

Aluminum alloys are the second most widely used metallic materials after steels. Their most important properties are:

- *Low density* (2.7 g cm^{-3}) which can lead to significant energy savings, especially in transportation applications
- *Good mechanical properties* offering optimum tensile strength
- *Good workability* permitting the most varied shapes to be produced
- *Good castability* with a variety of casting techniques (sand, mold, die-casting)
- *Good machinability*
- *Ease of joining* using all commonly applied techniques
- *Comparatively high corrosion resistance* thanks to the spontaneous formation of a strongly adherent passivating surface film in air
- Applicability of *different surface treatments*
- *High electrical and thermal conductivity*, especially of unalloyed aluminum
- *Good optical properties* depending on the degree of purity
- *Nonmagnetic*
- *Low absorption cross section* for thermal neutrons
- *Noncombustible*, nonsparking
- *No health risk* is associated with the use of aluminum and its alloys
- Excellent *recycling* properties.

| | | |
|--------|--|-----|
| 6.1 | Production of Aluminum | 158 |
| 6.2 | Properties of Pure Al | 158 |
| 6.2.1 | Physical Properties | 158 |
| 6.2.2 | Mechanical Properties | 160 |
| 6.2.3 | Chemical Properties | 160 |
| 6.3 | Aluminum Alloy Phase Diagrams | 161 |
| 6.3.1 | Binary Al-Based Systems | 161 |
| 6.3.2 | Ternary Al-Based Systems | 164 |
| 6.4 | Classification of Aluminum Alloys | 166 |
| 6.5 | Structure and Basic Mechanical Properties of Wrought Work-Hardenable Aluminum Alloys ... | 167 |
| 6.5.1 | Al-Fe-Si and Unalloyed Aluminum (1xxx) | 167 |
| 6.5.2 | Wrought Al-Mn (3xxx) | 167 |
| 6.5.3 | Wrought Al-Si (4xxx) | 167 |
| 6.5.4 | Wrought Al-Mg and Al-Mg-Mn (5xxx) | 167 |
| 6.6 | Structure and Basic Mechanical Properties of Wrought Age-Hardenable Aluminum Alloys | 168 |
| 6.6.1 | Wrought Al-Cu-Mg and Al-Cu-Si-Mn (2xxx) Alloys | 168 |
| 6.6.2 | Wrought Al-Mg-Si (6xxx) | 168 |
| 6.6.3 | Wrought Al-Zn-Mg and Al-Zn-Mg-Cu Alloys (7xxx) | 169 |
| 6.6.4 | Al-Zn-Mg-Cu Alloys | 170 |
| 6.7 | Structure and Basic Mechanical Properties of Aluminum Casting Alloys | 171 |
| 6.7.1 | Al-Si Casting Alloys | 171 |
| 6.7.2 | Al-Si-Mg Casting Alloys | 171 |
| 6.7.3 | Al-Mg Casting Alloys | 171 |
| 6.7.4 | Al-Zn-Mg Casting Alloys | 172 |
| 6.8 | Technical Properties of Aluminum Alloys | 173 |
| 6.8.1 | Mechanical Properties | 173 |
| 6.8.2 | Technological Properties | 177 |
| 6.8.3 | Physical Properties | 179 |
| 6.9 | Thermal and Mechanical Treatment ... | 181 |
| 6.9.1 | Work Hardening | 181 |
| 6.9.2 | Thermal Softening | 182 |
| 6.9.3 | Soft Annealing, Stabilization | 184 |
| 6.9.4 | Stress-Relieving | 184 |
| 6.9.5 | Homogenization | 185 |
| 6.9.6 | Aging | 185 |
| 6.9.7 | Effects of Plastic Deformation on Age-Hardening Behavior | 187 |
| 6.9.8 | Simultaneous Softening and Precipitation | 188 |
| 6.10 | Corrosion Behavior of Aluminum | 191 |
| 6.10.1 | Surface Layers | 191 |
| 6.10.2 | Corrosion | 192 |
| | References | 192 |

6.1 Production of Aluminum

The production of aluminum is based on the electrolysis of molten alumina (Al_2O_3) using the Hall–Héroult process. Alumina is extracted using the Bayer process from bauxite ore that contains 20–30 wt% Al. In 2016 the main producers of the ore are Australia (34%), China (25%), Brazil (13%), India (9%), Guinea (7%), and Jamaica (7%) [6.1, 2].

After milling, the ore is first broken down using an Al-containing NaOH solution that is seeded to precipitate aluminum hydroxide $\text{Al}(\text{OH})_3$. This is dehydrated at about 1100°C according to $2\text{Al}(\text{OH})_3 \rightarrow \text{Al}_2\text{O}_3 + 3\text{H}_2\text{O}$.

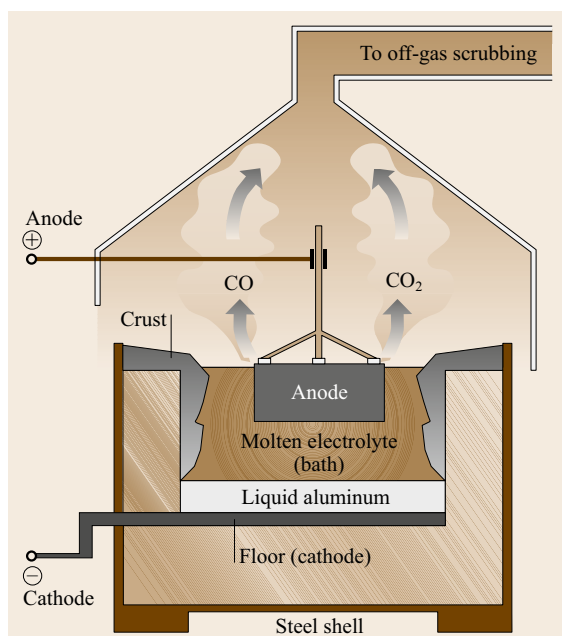


Fig. 6.1 Schematic representation of an electrolytic cell for Al production (after [6.1])

6.2 Properties of Pure Al

Aluminum can be classified as *unalloyed*, *pure*, or *refined* depending on its degree of purity. The Al from conventional electrolysis has a purity of 99.5–99.9 wt%. Higher purity is produced by *triple-layer refining electrolysis*, which can reach ≥ 99.99 wt% purity. The latter grade is used, for example, in the electronics sector.

6.2.1 Physical Properties

The physical properties of pure Al are given in Chap. 4, Tables 4.39–4.45. The temperature dependence of its

An electrolytic reduction is carried out in a cell as shown in Fig. 6.1. Cryolite Na_3AlF_6 is used as an additive to decrease the high melting point of pure Al_2O_3 (about 2050°C) as the two compounds form a eutectic near 10 wt% of Al_2O_3 in Na_3AlF_6 (Fig. 6.2) [6.3, 4]. The electrolysis is carried out in a cell lined with carbon, which serves as the cathode. Carbon anodes are suspended from above the cell into the electrolyte. Two main reactions occur: $2\text{Al}^{3+} + 6\text{e}^- \rightarrow 2\text{Al}$, and oxygen ions react with the carbon of the cathode to form CO_2 (consumption of the cathode). A primary aluminum smelter requires on average $13\text{--}14 \text{ kWh kg}^{-1}$ Al. In recent decades secondary production, i. e., recycling of scrap and waste material, has attained 30% of total production with high regional variations. Up to 95% less energy is needed to produce Al via secondary production.

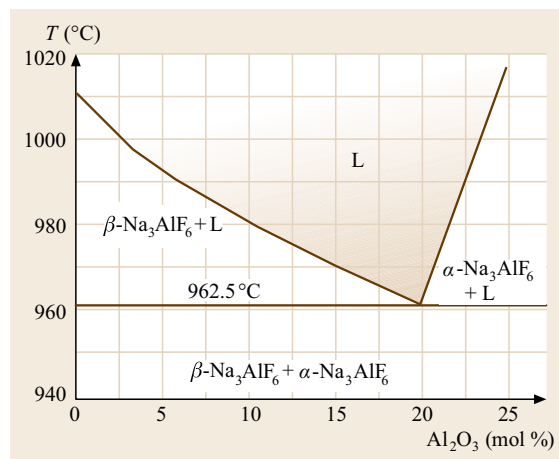


Fig. 6.2 Phase diagram of cryolite Na_3AlF_6 -alumina Al_2O_3 (after [6.1])

density is shown in Fig. 6.3. The contraction of 6.5% upon solidification corresponds to an increase in density from 2.37 g cm^{-3} in the liquid state to 2.55 g cm^{-3} in the solid state. The temperature dependence of the coefficient of thermal expansion is given in Table 6.1.

The specific heat in the solid state increases with temperature from 720 kJ at -100°C , to 900 kJ at 20°C , and 1110 kJ at 500°C . At its melting point Al has a specific heat of 1220 kJ (solid) and 1040 kJ (liquid). In the liquid state the specific heat rises further, e.g., to 1060 kJ at 800°C . Aluminum has a high re-

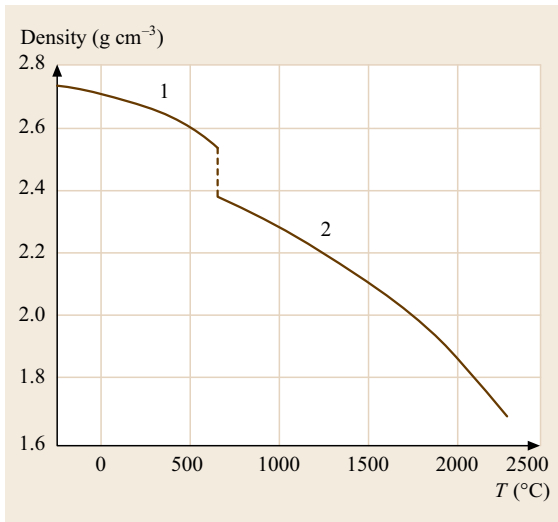


Fig. 6.3 Density of solid and liquid aluminum as a function of temperature (after [6.1])

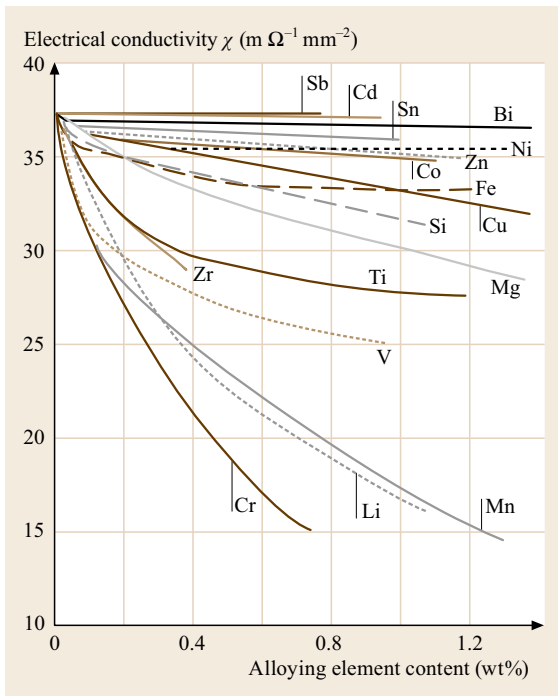


Fig. 6.4 Electrical conductivity of as-cast binary alloys based on high-purity aluminum as a function of the alloying element concentration (after [6.5, 6])

flexivity for light, heat, and electromagnetic radiation. The Young's modulus E of aluminum materials is usually taken to be 70 GPa; it varies between 60 and

Table 6.1 Coefficient of thermal expansion of Al 99.99 as a function of temperature (after [6.1])

| Temperature range (°C) | Average linear coefficient of thermal expansion (10^{-6} K^{-1}) |
|------------------------|--|
| (-200)–20 | 18.0 |
| (-200)–20 | 21.0 |
| 20–100 | 23.6 |
| 20–200 | 24.5 |
| 20–400 | 26.4 |
| 20–600 | 28.5 |

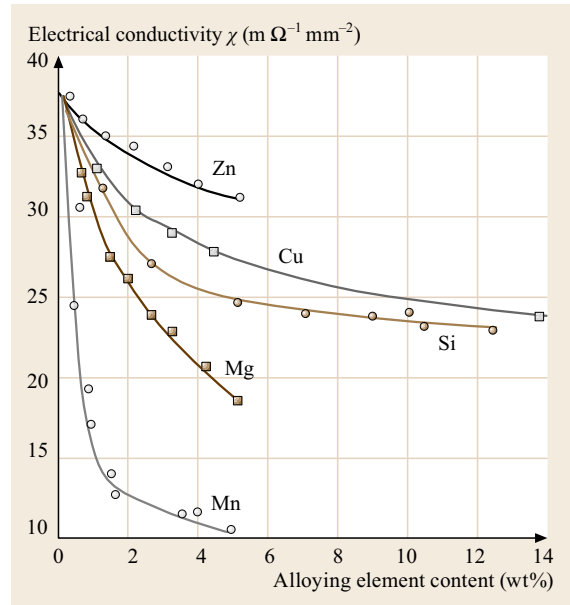


Fig. 6.5 Electrical conductivity of as-cast binary aluminum alloys (containing larger amounts of the alloying additions) as a function of concentration of the alloying element (after [6.5, 6])

78 GPa depending on alloy composition. The shear modulus G varies between 22 and 28 GPa, the value for refined aluminum is 25.0 GPa. Poisson's ratio ν varies between 0.32 and 0.40 (0.35 for refined aluminum).

Unalloyed aluminum has an electrical conductivity of $34\text{--}38 \text{ m}\Omega^{-1} \text{ mm}^{-2}$. Because of this relatively high conductivity, a large fraction of unalloyed Al and Al-Mg-Si alloys are used for electrical conductors. The temperature dependence of the electrical conductivity depends on alloying additions, impurities, and microstructure (Figs. 6.4–6.6). Superconductivity occurs at $T_c = 1.2 \text{ K}$ in refined grades of aluminum ($\geq 99.99 \text{ wt}\%$). The electrical conductivity of high-purity aluminum is still high at 4.2 K.

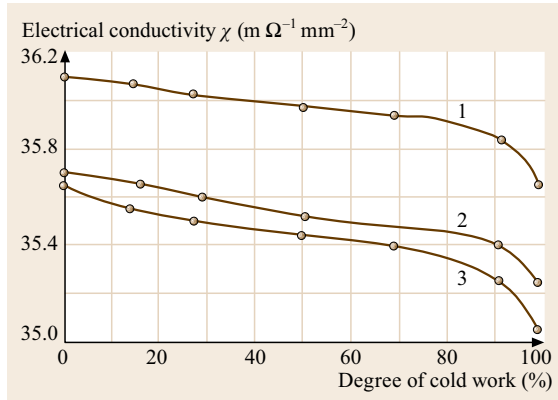


Fig. 6.6 Electrical conductivity of unalloyed Al (0.21 wt% Fe; 0.11 wt% Si) as a function of the degree of cold work and the degree of supersaturation and/or intermediate annealing temperature (after [6.5]): (1) intermediate annealing temperature 350 °C; (2) intermediate annealing temperature 500 °C; (3) as extruded

6.2.2 Mechanical Properties

The ultimate tensile strength of pure aluminum increases markedly with increasing amounts of alloying or impurity additions, as shown in Fig. 6.7. Unalloyed aluminum is soft (tensile strength 10–30 MPa, Table 6.2) and, like all fcc metals, shows a low rate of work hardening.

6.2.3 Chemical Properties

Aluminum, as a relatively reactive element, is a very strong base as shown by its position in the electrochemical series and its low standard potential ($V_H = -1.66$ V) [6.7]. Therefore, it is not possible to obtain the element from aqueous solutions by electrolysis. Similarly, it is not possible to obtain aluminum via a carbothermic reaction. In chemical compounds, aluminum is positively charged and trivalent (Al^{3+}). It reacts readily with hydrochloric acid and caustic soda, but less readily with sulfuric acid; dilute sulfuric acid does not attack aluminum. It is not attacked by cold

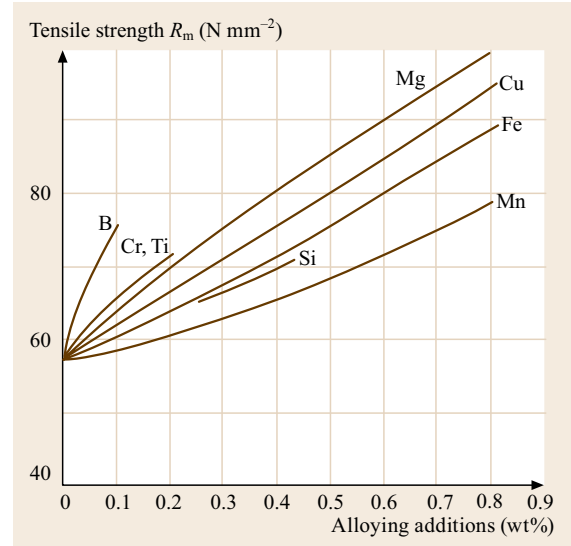


Fig. 6.7 Effect of small additions of alloying elements or impurities on the ultimate tensile strength of aluminum of high purity (99.98 wt% Al, soft condition, 5 h, 360 °C) (after [6.5])

nitric acid at any concentration, and hardly so when heated. The reaction with sodium hydroxide is given by: $2Al + 2NaOH + 3H_2O \rightarrow 2Na[Al(OH)_4] + 3H_2$.

Aluminum-based materials are nonflammable. Even turnings and chippings do not ignite. Extremely fine aluminum particles can undergo spontaneous combustion and thus cause explosions. The heat of formation of aluminum oxide Al_2O_3 is about 1590 kJ mol⁻¹, making aluminum a very effective deoxidizer for the steel industry and in metallothermic metal reduction processes (aluminothermy; e.g., $3V_2O_5 + 10Al \rightarrow 6V + 5Al_2O_3$ and aluminothermic welding, e.g., the *Thermite process* $3Fe_3O_4 + 8Al \rightarrow 9Fe + 4Al_2O_3$).

Important aluminum compounds include aluminum oxide Al_2O_3 , which is commonly called alumina (in powder form) or corundum (in coarse crystalline form), and aluminum hydroxide $Al(OH)_3$ (*hydrated alumina*, usually extracted from bauxite in the Bayer process).

Table 6.2 Typical mechanical properties of refined aluminum (Al 99.98) (after [6.1])

| Condition | Proof stress $R_{p0.2}$ (MPa) | Ultimate tensile strength R_m (MPa) | Elongation at fracture A_{10} (%) | Brinell hardness number HB |
|-----------|-------------------------------|---------------------------------------|-------------------------------------|----------------------------|
| Soft | 10–25 | 39–49 | 30–45 | 15 |
| Hard | 69–98 | 88–118 | 1–3 | 25 |

6.3 Aluminum Alloy Phase Diagrams

The properties of aluminum strongly depend on the concentration of alloying additions and impurities. Even the low residual contents of Fe and Si in unalloyed aluminum (Al 99–Al 99.9) have a marked effect.

The main alloying elements of Al materials are Cu, Si, Mg, and Zn while Mn, Fe, Cr, and Ti are frequently present in small quantities, either as impurities or additives. Ni, Co, Ag, Li, Sn, Pb, and Bi are added to produce special alloys. Be, B, Na, Sr, and Sb may be added as important trace elements. All of these elements affect the structure and thus the properties of an alloy. The compositions of the more important aluminum materials are discussed below, using the relevant phase diagram. All alloying components are completely soluble in liquid aluminum if the temperature is sufficiently high. However, these elements have only limited solubility in solid solution (Table 6.3). Continuous solid solubility does not occur in any of the alloy systems of Al.

Aluminum-rich solid solutions are often formed and are referred to as α -phase, α_{Al} -phase, or α -Al solid solution. Most of the phases occurring in equilibrium with α -Al are hard. They consist of elements or intermetallic compounds such as Al_2Cu , Al_8Mg_5 , Al_6Mn , Al_3Fe , and $AlLi$.

6.3.1 Binary Al-Based Systems

Aluminum–Copper

Al–Cu forms a simple eutectic system in the range from 0 to 53 wt% Cu, as shown in Fig. 6.8. The α -Al solid solution and the intermetallic compound Al_2Cu (θ -phase) are in equilibrium. At intermediate temperatures, metastable transition phases may form and precipitate from the supersaturated solid solution. These metastable phases may be characterized according to

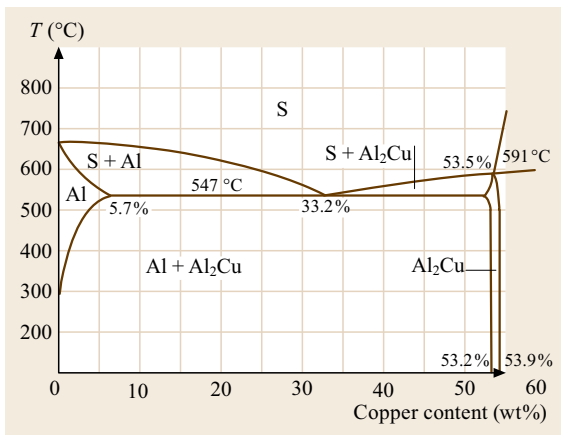


Fig. 6.8 Al– Al_2Cu section of the Al–Cu system (after [6.8])

their crystal structure, the nature of the phase boundary they form, and their size:

- From room temperature up to $\approx 150^\circ C$ the coherent Cu-rich Guinier–Preston I zones (GP I phase) form; they are only 1–2 {001} layers thick and have a highly strained, coherent phase boundary with the α -Al matrix phase.
- At ≈ 80 to $\approx 200^\circ C$ the GP II phase, also called θ'' -phase, forms; it has a superlattice structure based on the Al fcc lattice and has a coherent interface also, but the particle size grows larger than that of GP I.
- Above $\approx 150^\circ C$ the θ' -phase forms; it is only partially coherent.
- Above $\approx 300^\circ C$ the incoherent, stable θ -phase Al_2Cu is formed (overaging).

These phase transformations are decisive for the precipitation-hardening behavior of Al–Cu-based technical Al alloys.

Aluminum–Silicon

Al–Si forms a simple eutectic system (Fig. 6.9). At room temperature the solubility of Si in Al is negligible. Thanks to the good casting properties of the Al–Si eutectic, this alloy system forms the basis of a major part of the Al-based casting alloys. However, when slowly cooled (e.g., in sand casting), a degenerate form of eu-

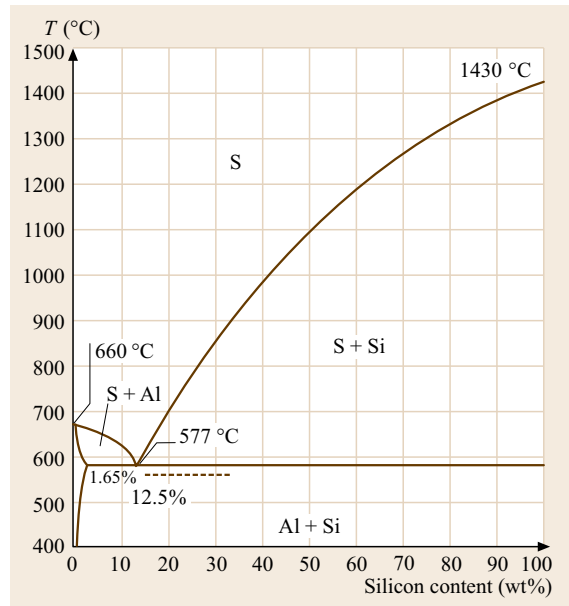
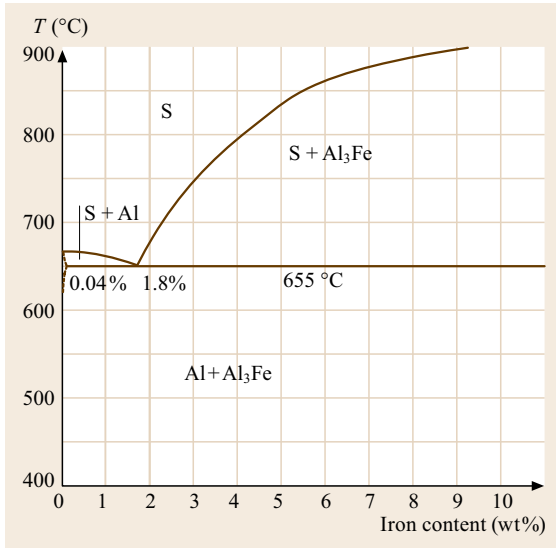
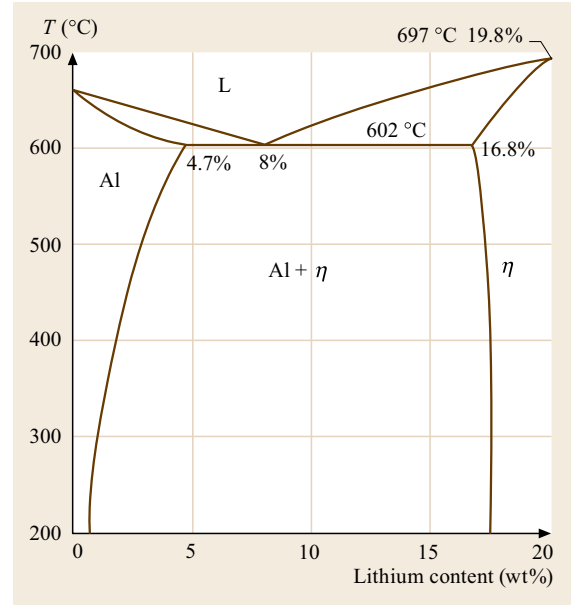
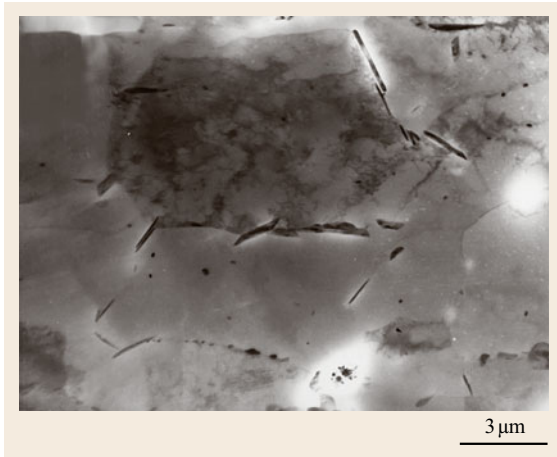


Fig. 6.9 Al–Si system; the dashed line shows the extent to which alloys can be supercooled (after [6.9])

Table 6.3 Solubility of some elements in aluminum solid solutions (after [6.8, 10])

| Element | Temperature of eutectic (E) or peritectic (P) equilibrium (°C) | Phase in equilibrium with Al solid solution | T_E or T_P (wt%) | Solubility (wt%) at | | | |
|---------|--|---|----------------------|---------------------|---------|--------|--------|
| | | | | 500 °C | 400 °C | 300 °C | 200 °C |
| Cu | 547 (E) | Al_2Cu | 5.7 | 4.4 | 1.6 | 0.6 | 0.2 |
| Fe | 655 (E) | Al_3Fe | ≈ 0.04 | 0.005 | < 0.001 | | |
| Li | 602 (E) | AlLi | 4.7 | 2.8 | 2.0 | 1.5 | 1.0 |
| Mg | 450 (E) | Al_8Mg_5 | 17.4 | ≈ 12.0 | 12.2 | 6.6 | 3.5 |
| Mn | 657 (E) | Al_6Mn | 1.82 | 0.36 | 0.17 | 0.02 | |
| Si | 577 (E) | Si | 1.65 | 0.8 | 0.3 | 0.07 | 0.01 |
| Zn | 275 Eutectoid equilibrium | Zn | 31.6 | | | | 14.5 |

**Fig. 6.10** Al-Fe system up to 10 wt% Fe**Fig. 6.12** Al-Li system for up to 20 wt% Li (after [6.10])**Fig. 6.11** Al_3Fe needles formed after annealing commercially pure aluminum sheet (Al 99.5) for 65 h at 590 °C, magnification 800 \times (after [6.11])

itectic microstructure may occur. Instead of the desired fine eutectic array, the alloy develops a structure that is characterized by larger, plate-like primary Si crystals, leading to very brittle behavior. This degenerate behavior can be suppressed by the addition of small amounts of Na, Sb, or Sr to the melt at about 720–780 °C. This *modification* causes a lowering of the eutectic temperature and a shift in concentration of the eutectic point, as indicated in Fig. 6.9; the extent of the shift is dependent on the rate of solidification.

Aluminum-Iron

Figure 6.10 shows the Al-rich part of this system. The solubility of Fe in Al is very low. In the range shown Al_3Fe is formed by a peritectic reaction at 1160 °C. The eutectic between the Al phase and Al_3Fe crystallizes in a degenerate manner to form brittle needles of Al_3Fe .

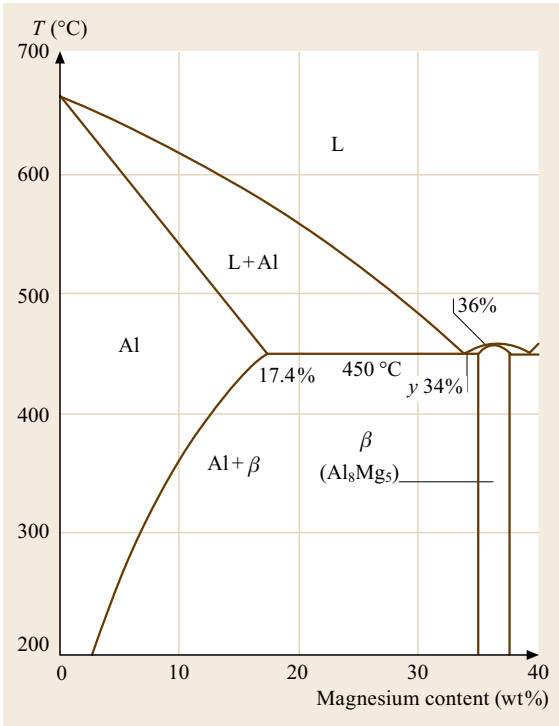


Fig. 6.13 Al- Al_8Mg_5 section of Al-Mg system (after [6.8])

The formation of Al_3Fe needles also occurs in Al-Fe-Si alloys such as commercially (available) pure aluminum (Fig. 6.11).

Aluminum-Lithium

The Al-rich part of this system is shown in Fig. 6.12. The Al(Li) solid solution and the η -phase (Al_3Li) are in

equilibrium. Al-Li-based alloys are used for their low density.

Aluminum-Magnesium

This system is shown in Fig. 6.13. The solid phases are the α -Al solid solution and the β - Al_8Mg_5 intermetallic compound. The high solubility of Mg in Al can be put to practical use for solid solution hardening. The β -phase precipitates preferentially at grain boundaries, forming a continuous network at the grain boundaries of the Al-rich α solid solution, e.g., after slow cooling from temperatures above 400 °C, especially in alloys containing more than 3 wt% Mg. Precipitates of the β -phase are less noble electrochemically than the α -phase and are thus subject to preferential attack by corrosive media. Accordingly the disadvantage of Al-Mg alloys is their potentially high susceptibility to intergranular corrosion.

Aluminum-Manganese

The Al-rich part of this system includes the intermetallic phases Al_4Mn (above 710 °C) and Al_6Mn (Fig. 6.14a). The α -Al solid solution and the Al_6Mn phase form a eutectic (Fig. 6.14b). The solubility of Mn in Al at room temperature is negligibly small. In hypereutectic Al-Mn alloys, precipitation of primary, bar-shaped Al_2Mn crystals occurs in the eutectic structure. These have a marked embrittling effect. Therefore, the maximum Mn content is limited to 2 wt% in commercial Al-Mn alloys.

Aluminum-Titanium

Intermetallic phases with a significantly higher melting point (dissociation temperature) than Al exist

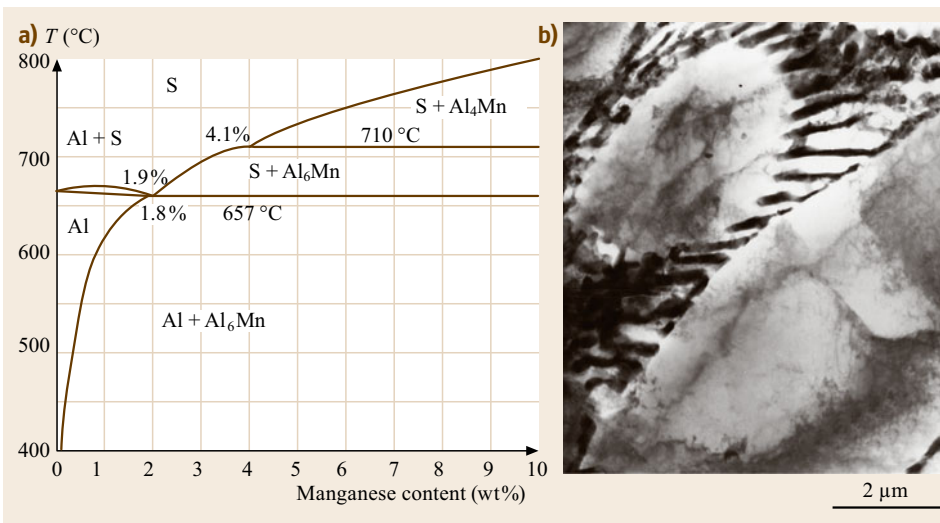


Fig. 6.14 (a) Al-Mn equilibrium system up to 10 wt% Mn. (b) Microstructure of an as-cast Al-1 wt% Mn alloy (TEM micrograph, magnification 7000 ×) (after [6.11])

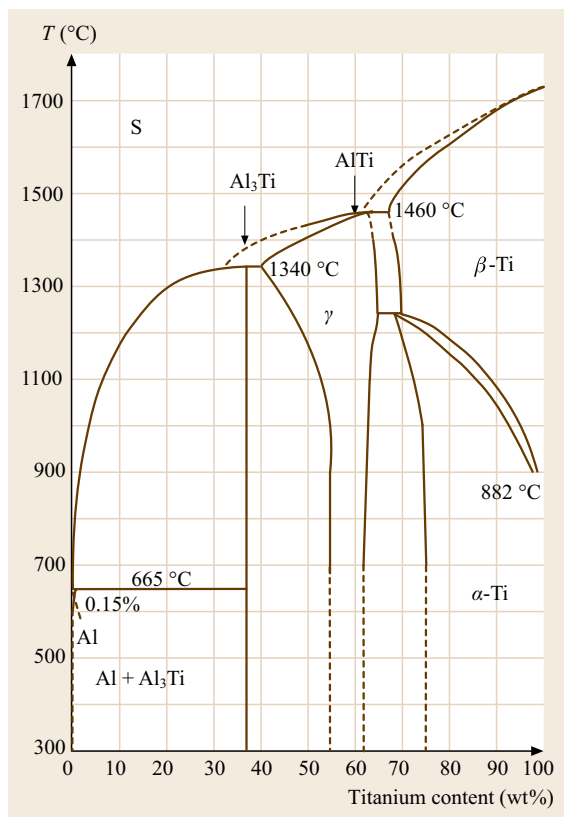


Fig. 6.15 Al-Ti system (after [6.8])

in this system: Al_3Ti (1340°C) and AlTi (1460°C) (Fig. 6.15). The structure of Al-rich Al-Ti alloys consists of Al_3Ti and an Al-rich solid solution.

Aluminum-Zinc

Zn is highly soluble in Al. The eutectic point occurs at a Zn-rich concentration (Fig. 6.16). The liquidus and solidus temperatures depend markedly on temperature.

6.3.2 Ternary Al-Based Systems

Most technical Al alloys contain more than two components because of the presence of impurity and alloying elements.

Aluminum-Iron-Silicon

Figure 6.17 shows the Al-rich corner as a section for 0.5 wt% Fe. This concentration range is of particular interest for commercially pure, unalloyed Al. Apart from the solid solution and the AlFe and Si phases there are two ternary phases, i. e., $\alpha\text{-Al}_{12}\text{Fe}_3\text{Si}$ and $\beta\text{-Al}_9\text{Fe}_2\text{Si}_2$. The exact compositions are subject to discussion and

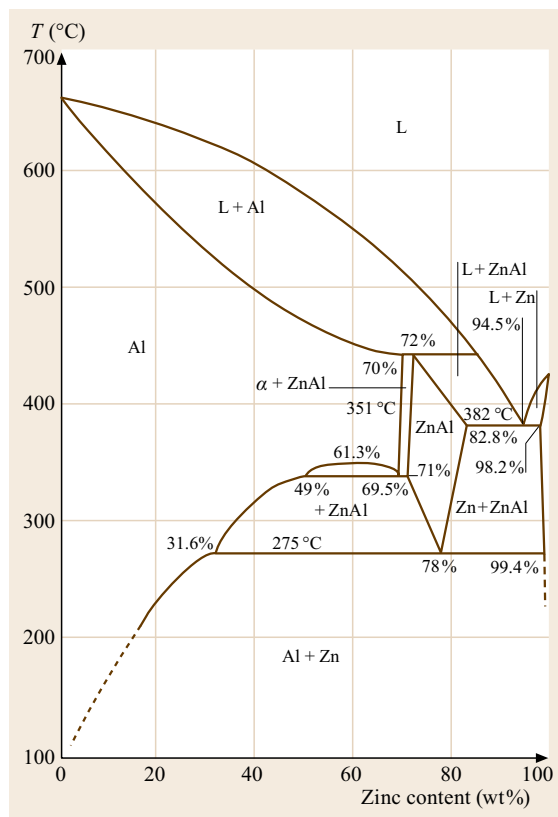


Fig. 6.16 Al-Zn system (after [6.8])

there are corresponding differences in the description of the solidification and precipitation processes. At the level of Fe and Si contents found in commercially pure aluminum ($\text{Al} + \text{Si} \leq 1 \text{ wt}\%$), $\alpha\text{-Al}_{12}\text{Fe}_3\text{Si}$ will form as a result of the transformation of the α -solid solution and AlFe with decreasing temperature, as shown in Fig. 6.11. If the temperature further decreases, precipitation of $\beta\text{-Al}_9\text{Fe}_2\text{Si}_2$ and even Si will occur. Because of the low rate of diffusion at low temperatures it is possible that all four phases coexist with the Al-rich solid solution phase. The solid solution becomes supersaturated in Fe and Si at the cooling rates used in industrial practice. Moreover, nonequilibrium ternary phases form, often locally at the grain boundaries of the as-cast microstructure. Fe and Si are in solution inside the grains. For a given cooling rate, the maximum Fe solubility decreases with increasing Si content of the alloy, whereas the Si solubility is independent of Fe content [6.12–14]. Thermodynamically, such nonequilibrium microstructures are very stable. The primary nonequilibrium ternary phases only decompose to the secondary equilibrium phases Al_3Fe and Si at about 600°C [6.15].

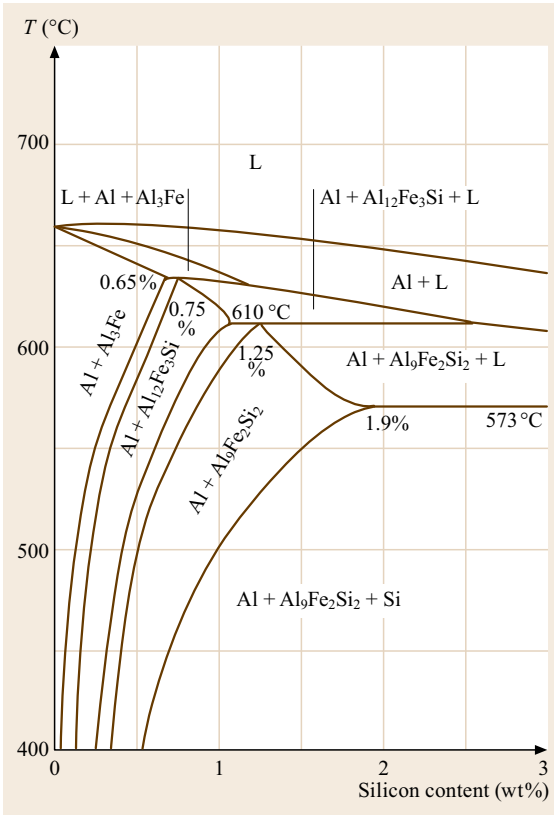


Fig. 6.17 Section through the Al-Fe-Si phase diagram at 0.5 wt% Fe (after [6.3]) ◀

Aluminum-Magnesium-Silicon

Figure 6.18a,b shows the Al-rich corner as a quasibinary section Al-Mg₂Si (Mg/Si ratio 1 : 0.58). It divides the system into the two simple ternary eutectic systems shown. The fine-grained microstructure of Al-Mg-Si alloys consists of α-Al(Mg,Si) and numerous intermetallic compounds, such as Mg₂Si (forming a characteristic particle shape called *Chinese script*), Al₆Mn, and Al₃Fe. Mg₂Si has an important effect on properties. Its solid solubility in the aluminum matrix is temperature-dependent and, thus, leads to hardening effects, which are exploited in technical alloys. A coarse network of intermetallic phases impairs forming behavior, but annealing before further processing produces finely dispersed precipitates. These improve workability but are, also, effective in retarding recrystallization.

Aluminum-Copper-Magnesium

In addition to the two binary phases, Al₈Mg₅ (β) and Al₂Cu (θ), there are two ternary phases, Al₂CuMg (S) and Al₆Mg₄Cu (T), in equilibrium with the Al-rich solid solution. The microstructure of castings shows various ternary eutectics which, in addition to Al₂Cu, also contain Mg₂Si, resulting from Si as an impurity, and AlCuMg [6.1].

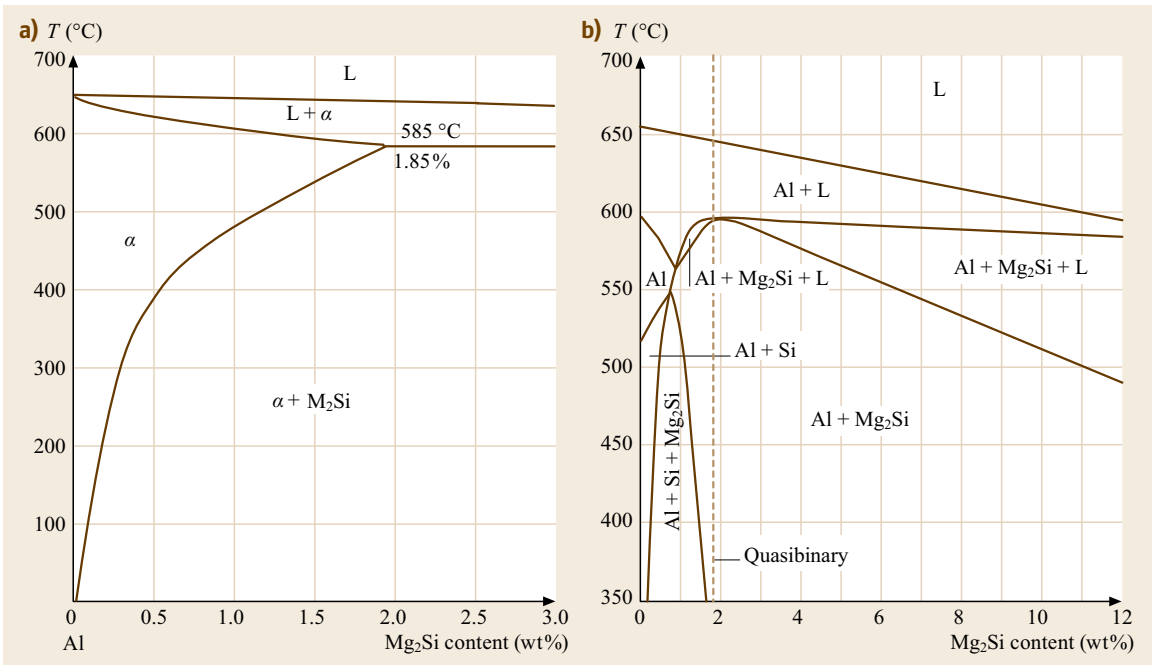


Fig. 6.18a,b Al-Mg-Si system. (a) Quasibinary section Al-Mg₂Si (after [6.8]); (b) section at a constant Si content of 1 wt% (after [6.3])

Aluminum-Copper-Lithium

In addition to binary phases between all three elements, three ternary phases, $\text{Al}_7\text{Cu}_4\text{Li}$, Al_2CuLi , and $\text{Al}_5\text{Li}_3\text{Cu}$ occur in equilibrium with the Al-rich solid solution in the aluminum-rich corner of this system.

Aluminum-Zinc-Magnesium

The Al-rich corner consists of two binary phases, Al_8Mg_5 and MgZn_2 , and a ternary phase T with a nominal composition $\text{Al}_2\text{Mg}_2\text{Zn}_3$ having a wide range of homogeneity. The Al-MgZn₂ and Al-T sections may be regarded as quasibinary systems with eutectic temperatures at 475 and 489 °C, respectively. The

Al- Al_8Mg_5 -T range constitutes a ternary eutectic, $T_E = 450^\circ\text{C}$. In the Al-T-Zn range there is a four-phase reaction in which the T phase transforms to Mg_2Zn . At high Zn contents, $\text{Mg}_2\text{Zn}_{11}$ transforms to MgZn_2 in another four-phase reaction at 365 °C. MgZn_2 subsequently solidifies eutectically at 343 °C together with Al and Zn. There is evidence of eutectic solidification in the as-cast structure of these alloys. If ternary Al-Zn-Mg alloys are solution-treated at temperatures above 450 °C they consist of a homogeneous α -phase solid solution that is supersaturated with respect to one phase at least, corresponding to its composition [6.1].

6.4 Classification of Aluminum Alloys

Technical aluminum alloys are subdivided first into the two main groups of cast and wrought alloys (Fig. 6.19). Typically, the alloying content of casting alloys is 10–12 wt%. This is significantly higher than the value for wrought alloys, most of which contain only a total of 1–2 wt% alloying elements; their content may be as high as 6 or even 8 wt% in individual cases.

Aluminum alloys are further subdivided, depending on whether or not an alloy can be hardened by the addition of alloying elements, as is the case with:

- Precipitation-hardenable alloys that can be strengthened by aging and
- Nonprecipitation-hardenable alloys that can be strengthened by work-hardening only.

The addition of further alloying elements will always cause hardening, but not all elements have the same hardening effect. Hardening will also depend on whether the solute atoms are present in solid solution or as particles. Alloy hardening can be divided into:

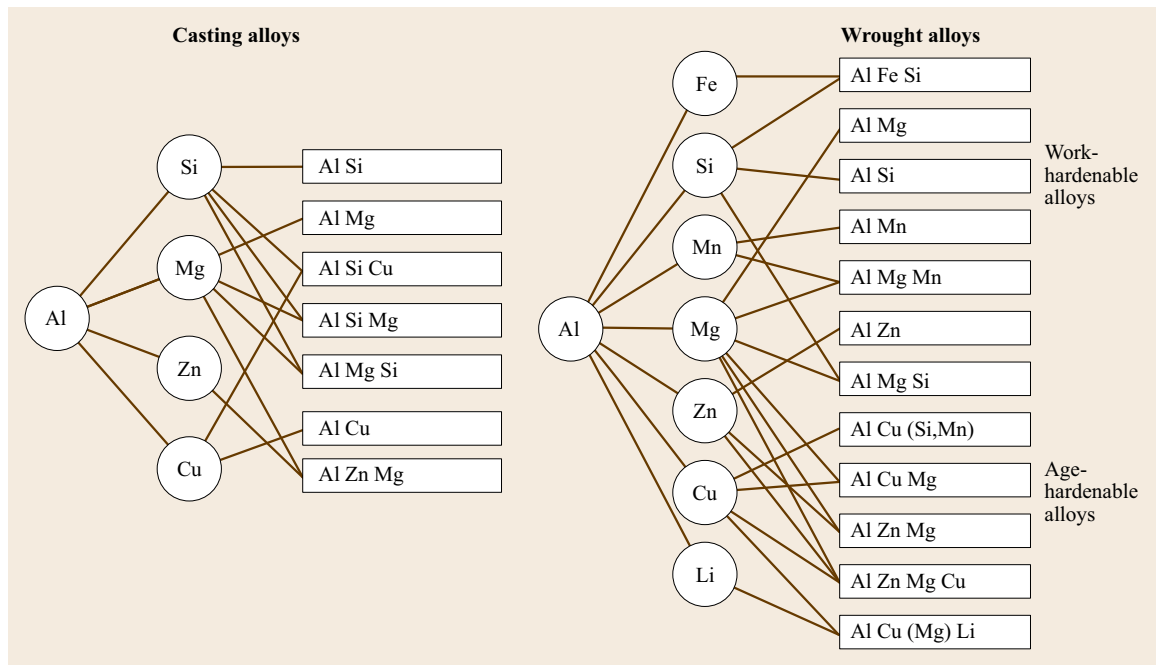


Fig. 6.19 Schematic array of cast and wrought aluminum alloys. The numbers are given according to European standardization. In the case of wrought alloys the numbers are the same as those used in North American standardization

- Solid-solution hardening (as with nonprecipitation hardening, work-hardenable alloys) and
- Hardening due to elements that are initially in solid solution and are precipitating as second phases (as is the case with age-hardenable alloys).

6.5 Structure and Basic Mechanical Properties of Wrought Work-Hardenable Aluminum Alloys

6.5.1 Al-Fe-Si and Unalloyed Aluminum (1xxx)

Al-Fe-Si contains about 0.6 wt% Fe and 0.8 wt% Si that has been added deliberately. The properties of Al-Fe-Si alloys, and of unalloyed aluminum, are strongly influenced by the elements that are in solid solution and the binary and higher phases that form. Increasing amounts of alloying additions lead to a marked increase in strength but there is a decrease in electrical conductivity since transition elements have a high effective scattering power for electrons.

6.5.2 Wrought Al-Mn (3xxx)

Manganese additions increase the strength of unalloyed aluminum (Fig. 6.20). The chemical resistance is not impaired. These alloys have very good forming properties when the Mn content is below the maximum solubility of Mn in the Al-rich α -phase, i. e., practically below 1.5 wt%. At higher Mn content, brittle Al_6Mn crystals form and impair workability.

If Al-Mn alloys are rapidly solidified as in continuous casting, considerable supersaturation of Mn occurs. Fe reduces the solubility for Mn and promotes its pre-

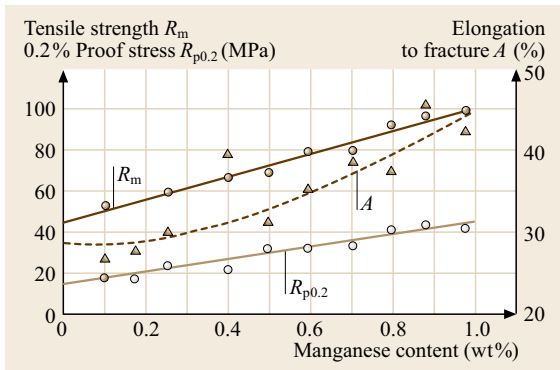


Fig. 6.20 Effect of manganese additions on the strength of aluminum; alloys based on 99.5 wt% Al, quenched from 565 °C, sheet samples, 1.6 mm thick (after [6.16])

It should be noted that age-hardenable alloys can be strengthened by the use of a suitable heat treatment whereas the same heat treatment of alloys that are not age-hardenable leads to a loss in strength.

precipitation in the form of multicomponent phases. Fe is often added to counteract supersaturation and for an increase of the tensile strength (Fig. 6.21). Depending on the amount of precipitation, Mn can inhibit recrystallization.

6.5.3 Wrought Al-Si (4xxx)

Aside from 1 to 12.5 wt% Si, wrought Al-Si alloys contain other elements such as Mg, Fe, Mn, or Cu.

6.5.4 Wrought Al-Mg and Al-Mg-Mn (5xxx)

The two nonage-hardening alloy systems Al-Mg and Al-Mg-Mn cover the entire compositional range from 0.5 to 5.5 wt% Mg, from 0 to 1.1 wt% Mn, and from 0

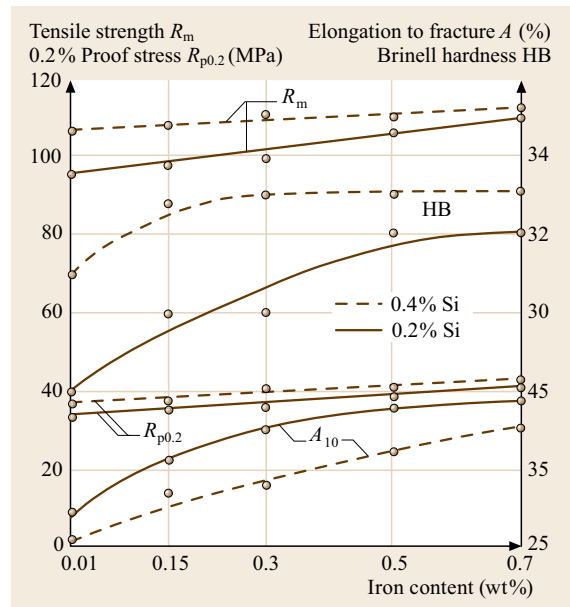


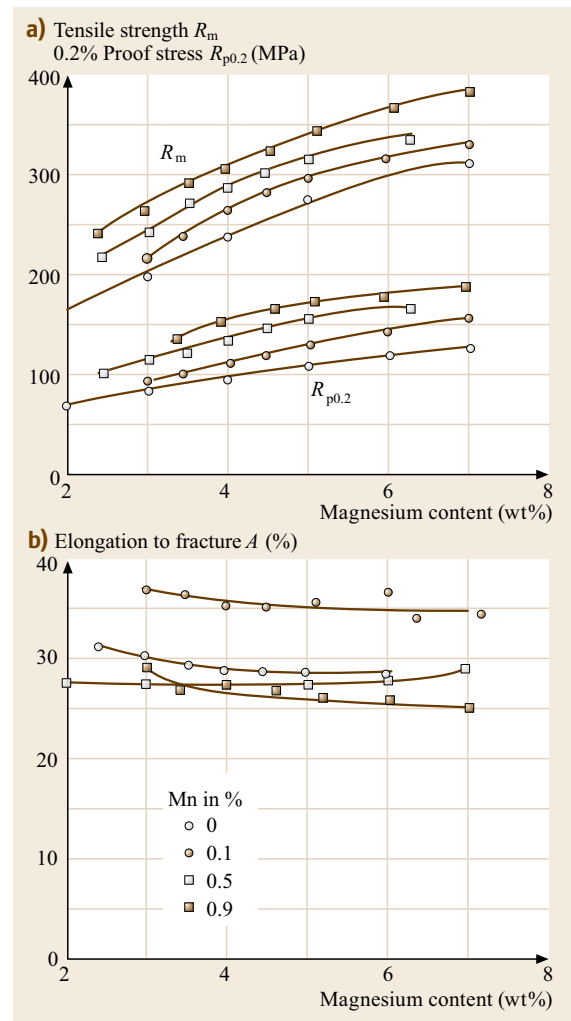
Fig. 6.21 Effect of iron and silicon on the strength of an Al-Mn alloy containing 1.2 wt% Mn; soft condition, sheet sample (after [6.17])

Fig. 6.22a,b Effect of Mn content on the mechanical properties of Al-Mg alloys: (a) tensile strength and 0.2% proof stress; (b) elongation to fracture (after [6.16]) ►

to 0.35 wt% Cr. Alloys with more than 5.6 wt% Mg are of no significance as wrought alloys.

In Al-Mg alloys both tensile strength and 0.2% proof stress increase with increasing Mg content, whereas elongation shows a steady decrease up to about 3 wt% Mg, beyond which it increases again slightly. Embrittlement does not occur at low temperatures. The solubility of Mg in the Al-rich solid solution decreases rapidly with decreasing temperature. Thus, most Al-Mg alloys are effectively supersaturated at room temperature. This is of practical significance in alloys containing more than 3 wt% Mg, where precipitation of the β -Al₃Mg₂ can occur, especially after prior cold working. This is not associated with any beneficial increases in strength but leads to deterioration in the corrosion resistance by intergranular corrosion (Fig. 6.13). It is necessary to avoid the formation of continuous networks of β particles at the grain boundaries. Individual β particles can be obtained by a globulization treatment (200–250 °C), followed by slow cooling.

Another means to increase strength is the addition of Mn. Al-Mn-Mg alloys show an additional increase in tensile strength, which is significantly higher than for binary Al-Mg alloys (Fig. 6.22). The alloys show good toughness and can be used at low temperatures. If the Mn content exceeds 0.6 wt%, the recrystallization temperature can be increased to such an extent that recrystallization does not occur during extrusion. With extruded sections, there is an increase in tensile strength and proof stress in the longitudinal direction termed the *press effect*.



6.6 Structure and Basic Mechanical Properties of Wrought Age-Hardenable Aluminum Alloys

6.6.1 Wrought Al-Cu-Mg and Al-Cu-Si-Mn (2xxx) Alloys

The 2xxx series alloys usually contain 3.5–5.5 wt% Cu and additions of Mg, Si, and Mn and residual Fe. They show a significant increase in tensile strength by aging (310–440 MPa). Natural (room temperature) or artificial aging (at elevated temperature) may be preferable, depending on the alloy composition (Fig. 6.23). Additions of up to 1.5 wt% Mg increase both tensile strength and proof stress. At these Mg contents, the Al-rich solid

solution is in equilibrium with the ternary Al₂CuMg phase which, together with the θ -phase (Al₂Cu), is responsible for hardening. Mn additions increase the strength (Fig. 6.24) and can also cause a press effect. For achieving good ductility, the Mn content is limited to ≈ 1 wt%.

6.6.2 Wrought Al-Mg-Si (6xxx)

Al-Mg-Si alloys are the most widely used wrought age-hardenable alloys. Hardening is attributable to the

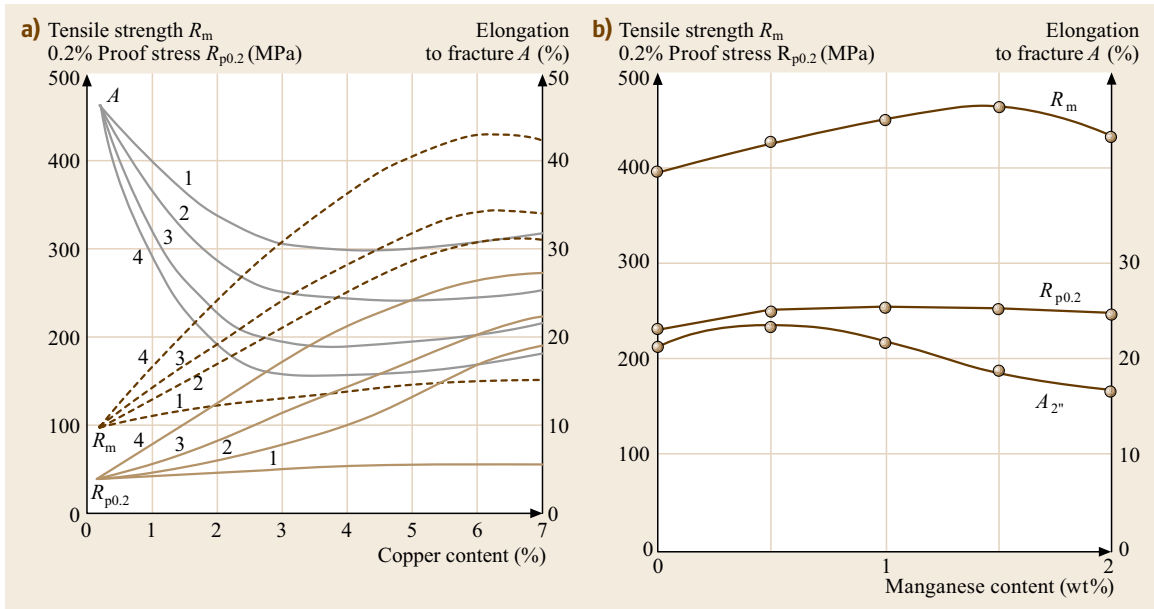


Fig. 6.23a,b Behavior of wrought Al-Cu-alloys. **(a)** Effect of copper on the strength of binary Al-Cu alloys; base material 99.95 wt% Al, 1.6 mm thick sheet (after [6.16]): (1) soft annealed; (2) solution annealed and quenched; (3) naturally aged; (4) artificially aged. **(b)** Effect of Mn on the strength of an Al-Cu-Mg alloy with ≈ 4 wt% Cu and 0.5 wt% Mg; naturally aged (after [6.16])

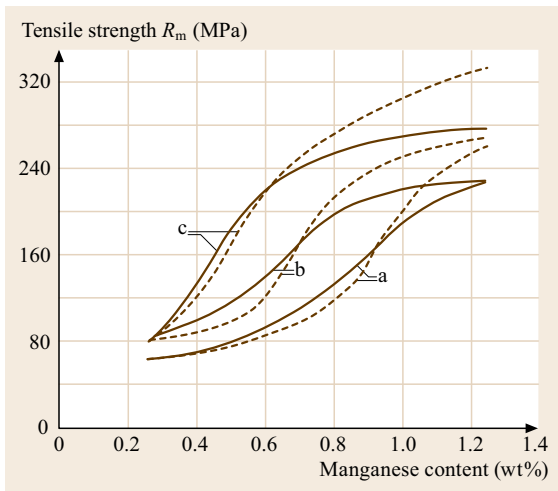


Fig. 6.24 Effect of Mg_2Si on tensile strength (after [6.1]): (a) stoichiometric composition, (b) 0.3 wt% excess Mg, (c) 0.3 wt% excess Si. The solid line refers to alloys that were quenched + immediate aging at 160 °C, the dashed line represents data for alloys that were quenched + intermediate aging for 24 h at 20 °C + aging at 160 °C

formation of the Mg_2Si phase. The compositional range of interest is 0.30–1.5 wt% Mg, 0.20–1.6 wt% Si, up to 1.0 wt% Mn, and up to 0.35 wt% Cr. This is equivalent to about 0.40–1.6 vol% Mg_2Si and varying

amounts of free Si and/or Mg. Some alloys are close to the pseudobinary section Al- Mg_2Si , in others there is a significant excess of Si. This affects the maximum attainable strength values because of the resulting variations in the amount of Mg_2Si , as shown in Fig. 6.25 for the quenched and artificially aged condition. Additions of 0.2–1.0 wt% Mn lead to an increase in the notch impact toughness of Al-Mg-Si alloys (Fig. 6.26), and affect the recrystallization behavior. Additions of Cr cause similar effects.

6.6.3 Wrought Al-Zn-Mg and Al-Zn-Mg-Cu Alloys (7xxx)

Additions of Zn to Al lead to an insignificant increase in strength. Combined additions of Zn and Mg cause age hardening and thus an increase in strength (Figs. 6.25 and 6.26). The sum of the Zn and Mg contents is limited to about 6–7% because of the risk of stress corrosion cracking at higher levels in Cu-free Al-Zn-Mg alloys; this results in medium strength. Zr, Mn, and Cr are added to reduce the tendency to recrystallize. If suitably heat-treated, such alloys have adequate corrosion resistance. It is important that cooling after solution treatment is not too rapid and that the proper precipitation treatment, usually step aging, is used. The alloys are of interest for welded structures because of their low quench sensitivity. The low-strength heat-affected

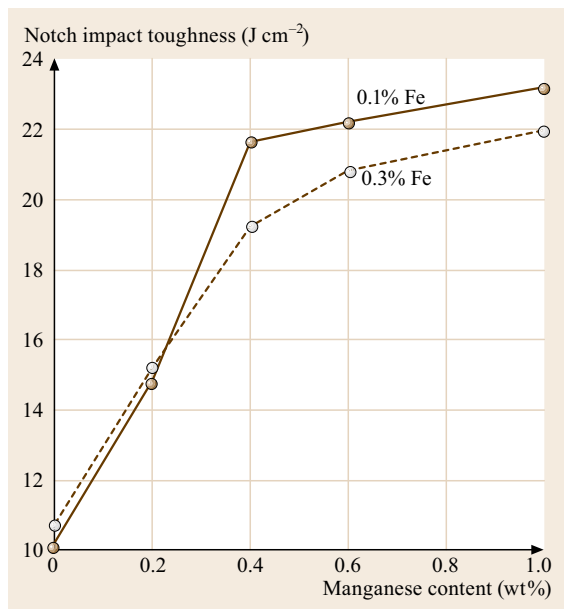


Fig. 6.25 Effect of Mn and Fe on the notch impact toughness of EN AW-AlSi1MgMn (former AlMgSi1) Al-alloy with 1 wt% Si and 0.75 wt% Mg; artificially aged, flat bars, $60 \times 10 \text{ mm}^2$ (after [6.17])

zone formed during welding is restored to full hardness without the need for renewed solution treatment. Al-Zn-Mg alloys usually contain 0.1–0.2 wt% Zr and some Ti in order to improve their weldability and resistance to stress corrosion cracking. Cu additions are avoided, despite their favorable effect on stress corrosion cracking, because they increase susceptibility to weld cracking.

6.6.4 Al-Zn-Mg-Cu Alloys

The addition of 0.5–2.0 wt% Cu strengthens Al-Zn-Mg alloys. Cu also reduces the tendency for stress corrosion cracking so that the upper limit for (Zn + Mg) can be increased to 9 wt%, provided additions of Cr are also made. The Zn/Mg ratio should preferably lie between 2 and 3. Al-Zn-Mg-Cu alloys can be aged both naturally and artificially. They attain the highest strength levels of all aluminum alloys. The actual hardening mechanism is attributable to Mg and Zn. Cu increases the rate of aging and acts as a nucleus for the hardening phases. Figure 6.27 shows some properties as a function of the Zn content at constant Cu content and two different Mg contents.

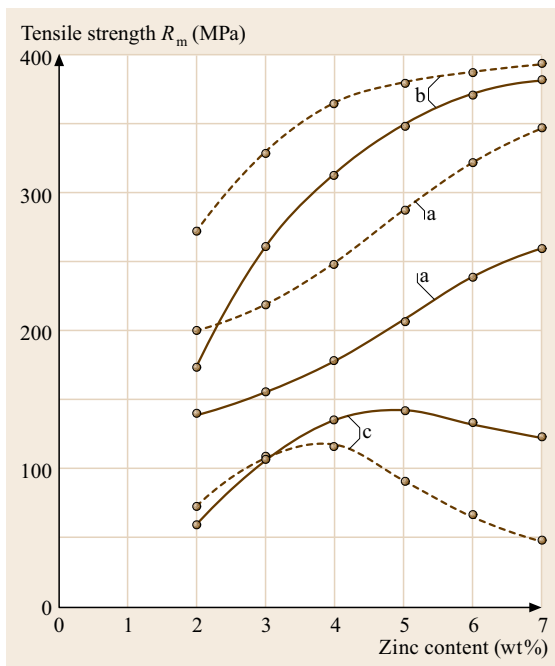


Fig. 6.26 Effect of Zn and Mg on the strength and aging effect of Al-Zn-Mg alloys (after [6.17]): (a) solution treatment at 450°C and quenching, (b) solution treatment at 450°C and quenching plus natural aging for 3 months, (c) aging effect, i. e., the increase in strength attributable to natural aging; difference between (a) and (b)

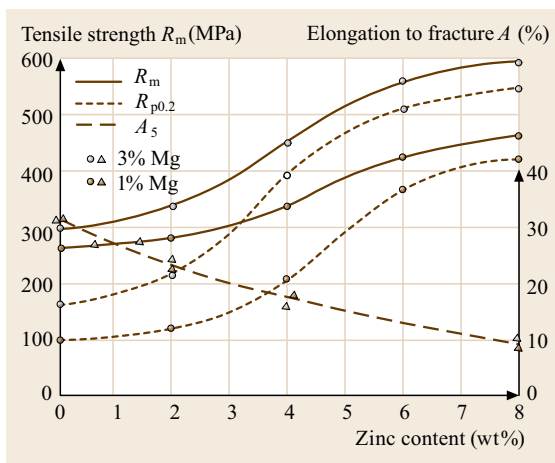


Fig. 6.27 Effect of zinc on the tensile properties of Al-Zn-Mg-Cu alloys; solution treated at 460°C , quenched, aged for 12 h at 135°C , 1.5 wt% Cu (after [6.16])

6.7 Structure and Basic Mechanical Properties of Aluminum Casting Alloys

6.7.1 Al-Si Casting Alloys

Because of the Al-Si eutectic (Fig. 6.9), these alloys, containing 5 to ≤ 20 wt% Si, have good casting properties. The tensile strength increases with the Si content (Fig. 6.28). Apart from Si other elements may be added, e.g., for the modification of the eutectic. Cu is present in residual amounts and impairs chemical resistance if levels exceed 0.05 wt%. Additions of about 1 wt% Cu yield an increase in solid solution hardening and thus reduce the tendency for smearing during machining. Residual Fe reduces sticking tendency, but leads to the formation of β -AlFeSi needles that reduce strength and ductility. Therefore, the Fe content must be limited. An addition of Mn has a favorable effect on the sticking tendency. Mn leads to the formation of a quaternary phase, but it poses no problem because of its globular shape. *Piston alloys* have hypereutectic compositions of up to 25 wt% Si. During solidification, primary Si crystals are formed that increase wear strength and reduce thermal expansion.

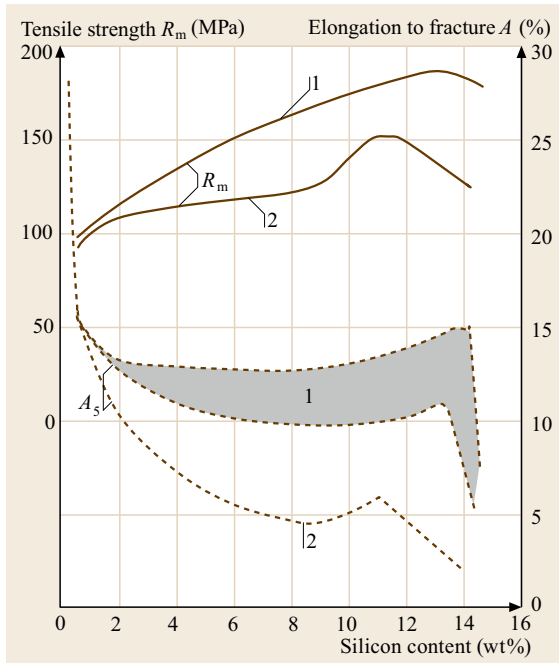


Fig. 6.28 Effect of Si on the strength and ductility of Al-Si casting alloys; (1) modified and (2) unmodified sand castings (after [6.1])

6.7.2 Al-Si-Mg Casting Alloys

These alloys contain about 5, 7, or 10 wt% Si and between 0.3 and 0.5 wt% Mg. The optimum amount of Mg decreases with increasing Si content. Mg causes high strength and a moderate ductility depending on the temper (Fig. 6.29). The alloys can be age hardened both naturally and artificially. Fe leads to a reduction in sticking tendency, but also to a drastic reduction in ductility.

6.7.3 Al-Mg Casting Alloys

These alloys contain 3–12 wt% Mg. Strength increases with increasing Mg content (Fig. 6.30). Above about 7 wt% Mg, the alloy has to be heat-treated to homogenize the structure and thus obtain good tensile properties. With Mg contents of up to 5 wt%, Si additions of up to 1 wt% are possible, and these lead mainly to improvements in the casting properties. The addition of Si causes hardening due to the formation of Mg_2Si .

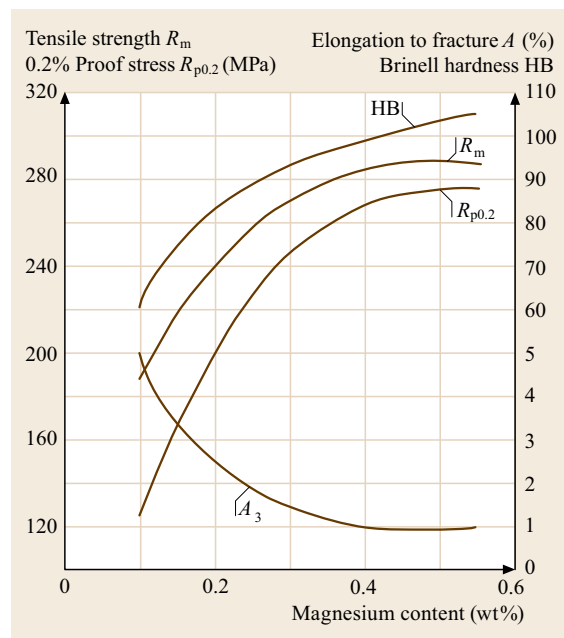


Fig. 6.29 Effect of Mg on the mechanical properties of EN AC-Al Si10Mg casting alloy (with 9.5 wt% Si, 0.45 wt% Fe, and 0.3 wt% Mn), sand cast and artificially aged (after [6.18–20])

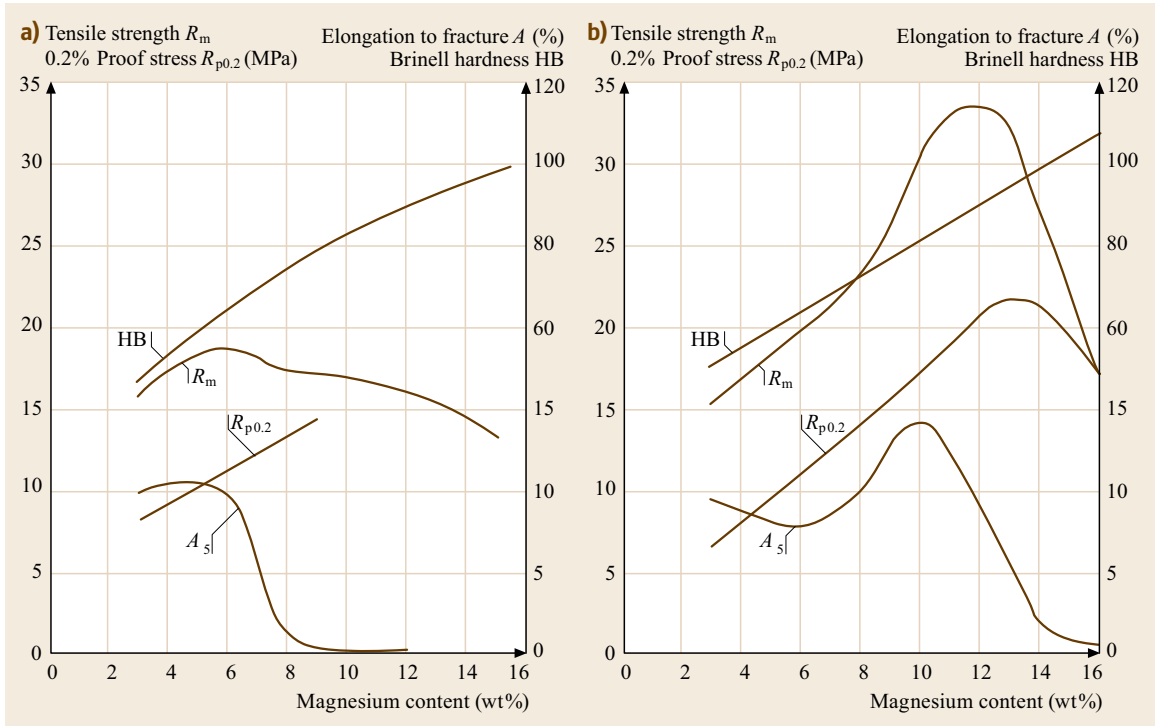


Fig. 6.30a,b Effect of Mg on the mechanical properties of Al-Mg casting alloys, sand cast, untreated and homogenized (after [6.1]): **(a)** as-cast condition, **(b)** homogenized

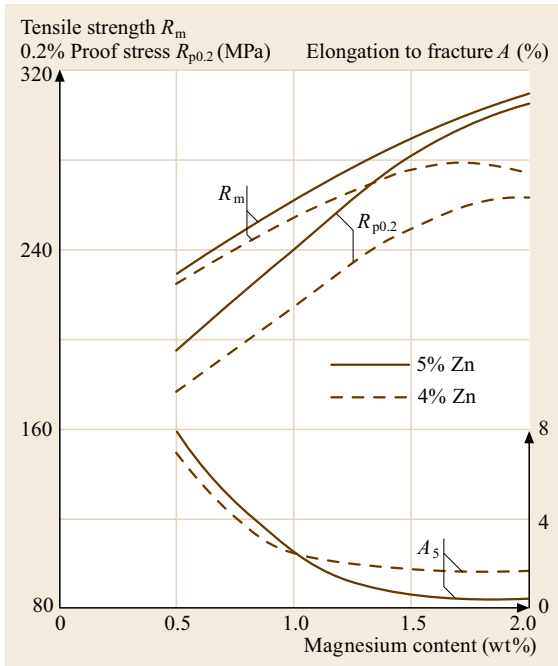


Fig. 6.31 Effect of Mg on the strength of cast Al-Zn-Mg alloys; sand casting, artificially aged (after [6.1])

6.7.4 Al-Zn-Mg Casting Alloys

They contain 4–7 wt% Zn and 0.3–0.7 wt% Mg. They can be naturally or artificially age hardened in the as-cast condition, without the need for prior solution treatment. Mg has a significant effect on the mechanical properties in the aged condition (Fig. 6.31). If the Mg content is limited, Al-Zn-Mg casting alloys can exhibit particularly good elongation to fracture.

6.8 Technical Properties of Aluminum Alloys

The applications of aluminum and its alloys are dependent on the properties. In most cases, mechanical properties are an important criterion for assessing the suitability of an Al alloy for a specific application. Other properties, such as electrical conductivity or corrosion resistance, may also be included in the assessment process.

6.8.1 Mechanical Properties

Hardness

The Brinell hardness number HB ranges from 15 for unalloyed Al in the soft temper to about 140 for an artificially aged Al-Zn-Mg-1.5 wt% Cu alloy.

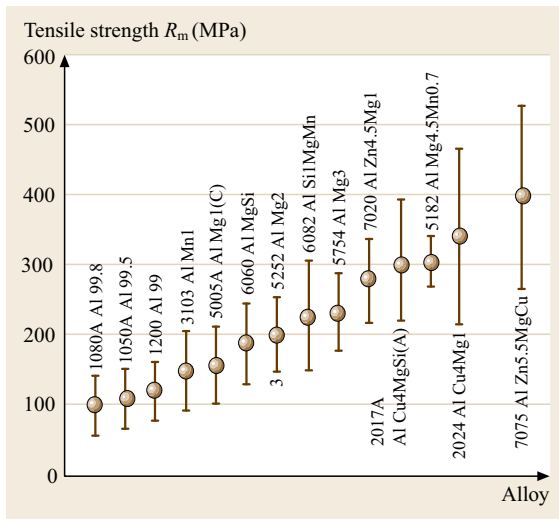


Fig. 6.32 Ranges of tensile strength for some important wrought aluminum alloys EN AW- (after [6.1])

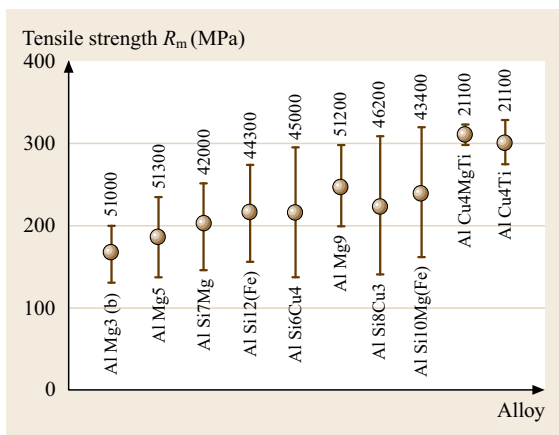


Fig. 6.33 Ranges of tensile strength for some important aluminum casting alloys EN AC- (after [6.1])

Tensile Strength

Figures 6.32 and 6.33 indicate the typical levels of strength attainable with wrought and cast aluminum alloys, respectively. There will be a range of tensile strengths in specific alloying systems because of possible additional increases in strength due to hardening by cold work or precipitation. The different alloying elements cause differing degrees of strengthening.

Strength at Elevated Temperatures

An example of the temperature and time dependence of the different mechanical properties is given in Fig. 6.34. With regard to the resistance to softening the materials can be classified as follows, depending on their temper:

- Wrought alloys in the soft temper and as-cast nonage-hardenable casting alloys are all practically thermally stable.
- For cold-worked wrought alloys, partially annealed to obtain an intermediate temper, the increase in strength due to forming is diminished with increasing temperature and exposure time.
- Artificially aged alloys do not undergo any permanent changes on annealing until approaching the aging temperature. At higher temperatures, aging continues from the point where it was interrupted during the aging process (Figs. 6.35 and 6.36).

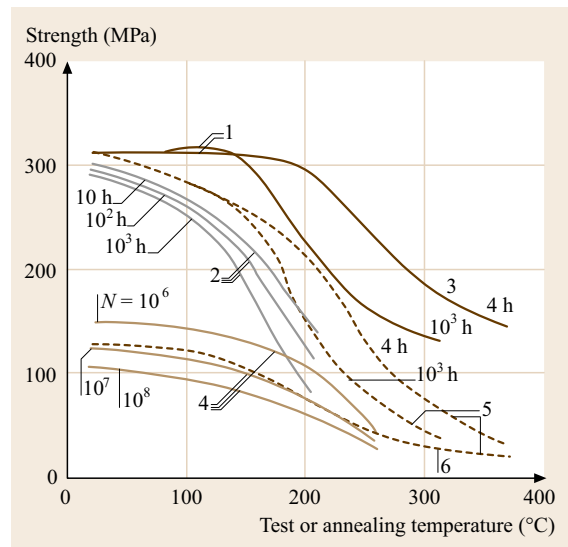


Fig. 6.34 Properties of EN AW-AlMg1SiCu 6061-T6 at elevated temperatures; 1.0 wt% Mg, 0.6 wt% Si, 0.3 wt% Cu, 0.25 wt% Cr, artificially aged (after [6.1]): (1) tensile strength R_m at 20 °C, (2) stress rupture strength, (3) duration of exposure, (4) fatigue strength, (5) tensile strength at test temperature, (6) solution treated

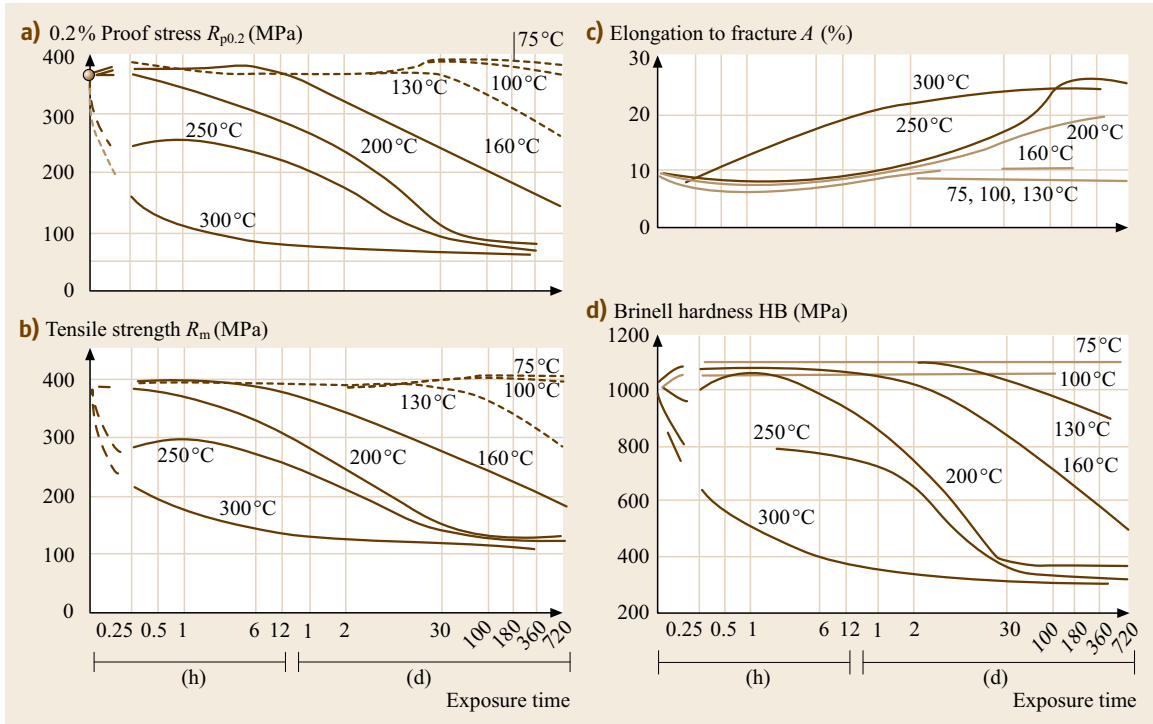


Fig. 6.35a–d Effect of temporary exposure to elevated temperature on the mechanical properties of artificially aged EN AW-Al Si1MgMn (6082) at 20 °C (after [6.1]): (a) 0.2% proof stress; (b) tensile strength; $R_{p0.2}$; (c) elongation to fracture A ; (d) Brinell hardness

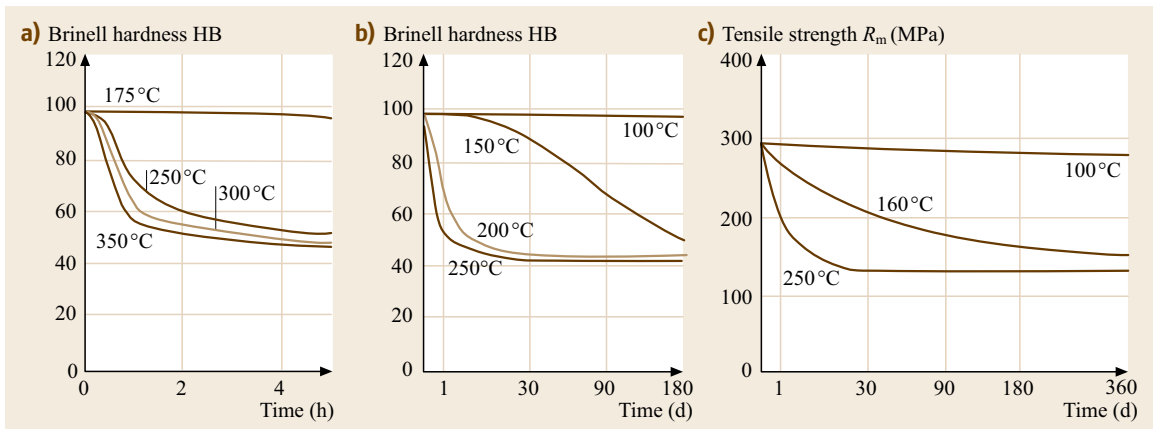


Fig. 6.36a–c Effect of temporary exposure to elevated temperature on the hardness and tensile strength at 20 °C of cast EN AC-Al Si10Mg(a) (43000) alloy, artificially aged (after [6.21]). (a) 0–4 h; (b) 1–180 d; (c) 1–360 d

- Naturally aged alloys usually exhibit increased hardening when exposed to higher temperatures as a result of artificial aging. At higher temperatures, the behavior is similar to that of artificially aged alloys.

High-Temperature Mechanical Properties in Short-Term Tests

In materials that are not thermally stable, there will be an effect due to irreversible changes in properties. Its magnitude depends on the temperature and duration of exposure (Figs. 6.37 and 6.38).

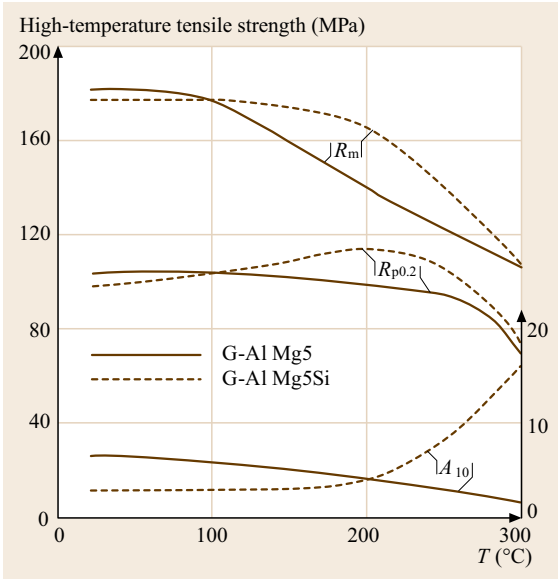


Fig. 6.37 High-temperature tensile strength of EN AC-Al Mg5 (51300) and EN AC-Al Mg5(Si) (51400) casting alloys, sand cast, after 30 min prior exposure to the test temperature (after [6.22])

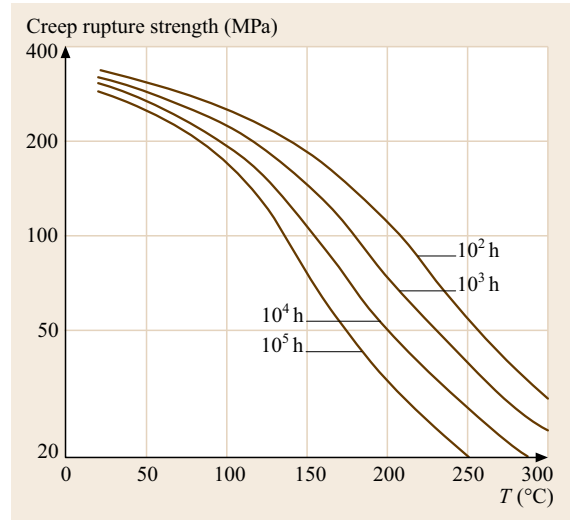
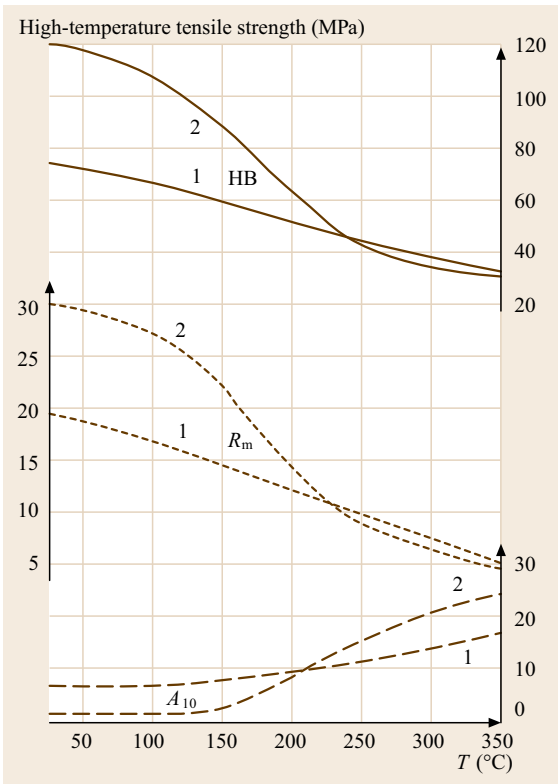


Fig. 6.39 Creep rupture behavior of EN AC-Al Si1MgMn (6082), T6 alloy, strain-hardened, min. tensile strength 320 MPa; extruded rods, 25 mm diameter (after [6.23, 24])

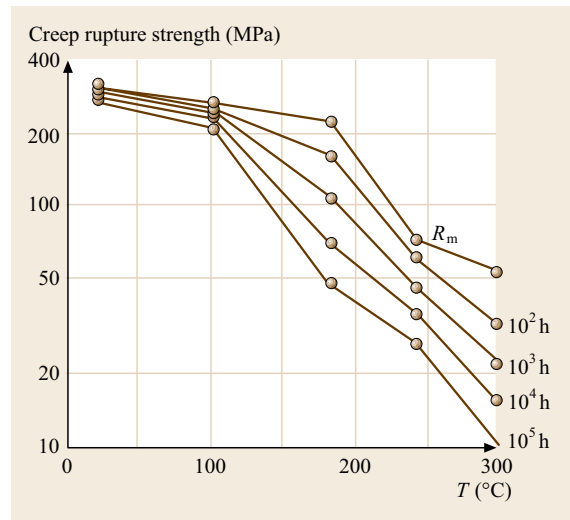


Fig. 6.40 Creep rupture behavior of EN AC-Al Si10Mg(a) (43000) casting alloy, artificially aged, 100 h prior exposure to the test temperature (after [6.23, 24])

Creep Behavior

Creep of Al alloys starts to play an important role at temperatures above 100–150 $^{\circ}\text{C}$ (Figs. 6.39 and 6.40).

Fig. 6.38 High-temperature tensile strength of casting alloys (after [6.21]): (1) as-cast EN AC-Al Si12(Fe) (44300); (2) EN AC-Al Si10Mg(a) (43000) after preheating for 8 d at the test temperature ◀

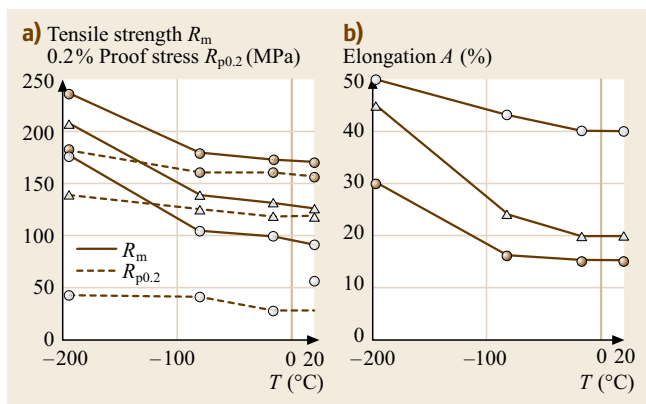


Fig. 6.41a,b Mechanical properties of unalloyed aluminum AA 1100 (Al 99) at low temperatures (after [6.1]): (a) tensile strength R_m and 0.2% proof stress $R_{p0.2}$; (b) elongation A

Material, amount of cold work, and degree of age-hardening can affect creep behavior in various ways. With nonage-hardenable alloys, the effect of cold working is more pronounced at low temperatures, below about 150°C. At higher temperatures, the behavior rapidly approaches that of the softened material. Thus, more highly alloyed materials in the soft temper may exhibit better creep properties than cold-worked alloys that are less highly alloyed. Artificially aged alloys should only be exposed for prolonged periods to temperatures that are significantly lower than the temperature of artificial aging, otherwise overaging will lead to a complete loss of strength.

Mechanical Properties at Low Temperatures

On the basis of its fcc crystal structure, Al and its alloys show neither a rapid increase in yield stress nor a rapid decrease in fracture toughness with decreasing temperature (Figs. 6.41–6.43). Tests carried out on Al-Mn, Al-Mg, Al-Mg-Si, Al-Cu-Mg, and Al-Zn-Mg wrought alloys at -268°C showed that the values of elongation to fracture at extremely low temperatures were even higher than at room temperature. In most cases, tensile strength and 0.2% proof stress increased weakly with decreasing temperature. Casting alloys behave similarly to wrought alloys at low temperatures. The behavior will depend on composition, temper (especially size, shape, and distribution of precipitates), and on the casting process used (Fig. 6.44).

Fatigue

Composition, heat treatment, and method of processing has a marked effect on fatigue strength. Solid solution hardening, cold work, and age hardening all lead to an increase in fatigue strength. For a given alloy composition, extruded sections usually have a higher fatigue strength than sheet or forgings. Fine grains are generally beneficial whereas coarse grains and coarse intermetallic phase particles can lead to a reduction in fatigue strength. Often there is an increase in fatigue strength with decreasing sample thickness, especially with bending stresses. Moreover, the effect of roughness or surface defects in thin specimens is usually less than that in thicker samples. With wrought aluminum alloys, there is a marked difference between

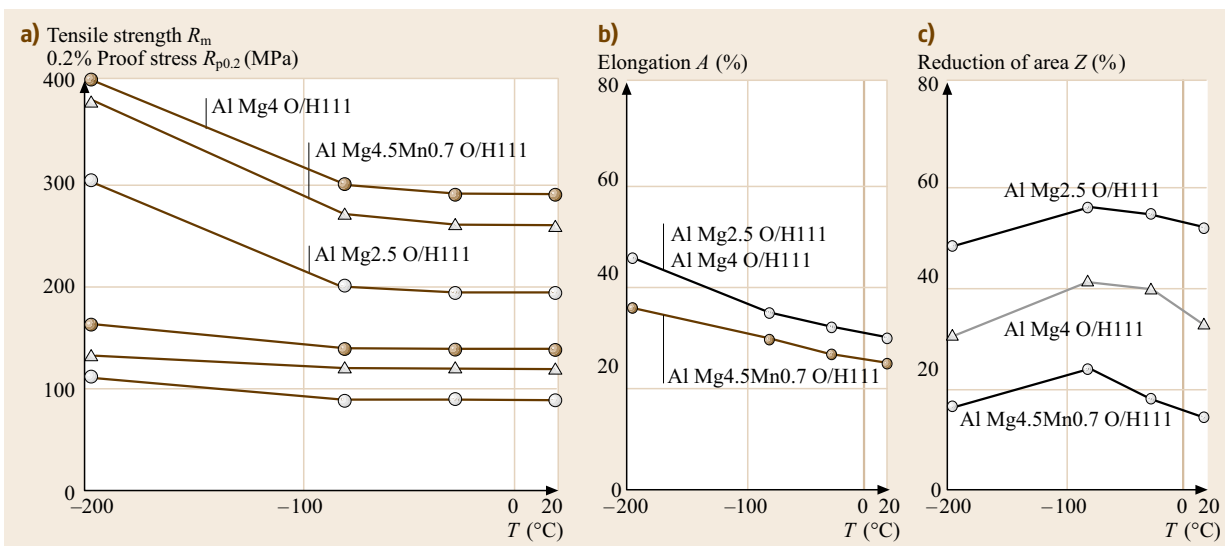


Fig. 6.42a–c Mechanical properties at low temperatures for some Al-Mg and Al-Mg-Mn alloys in the soft temper (after [6.1]). (a) Tensile strength R_m and 0.2% proof stress $R_{p0.2}$; (b) elongation $A_{2\sigma}$; (c) reduction of area alloys EN AW-5086 (Al Mg4), EN AW-5052 (Al Mg2.5), and EN AW-5083 (Al Mg4.5Mn0.7), all in soft temper O/H111

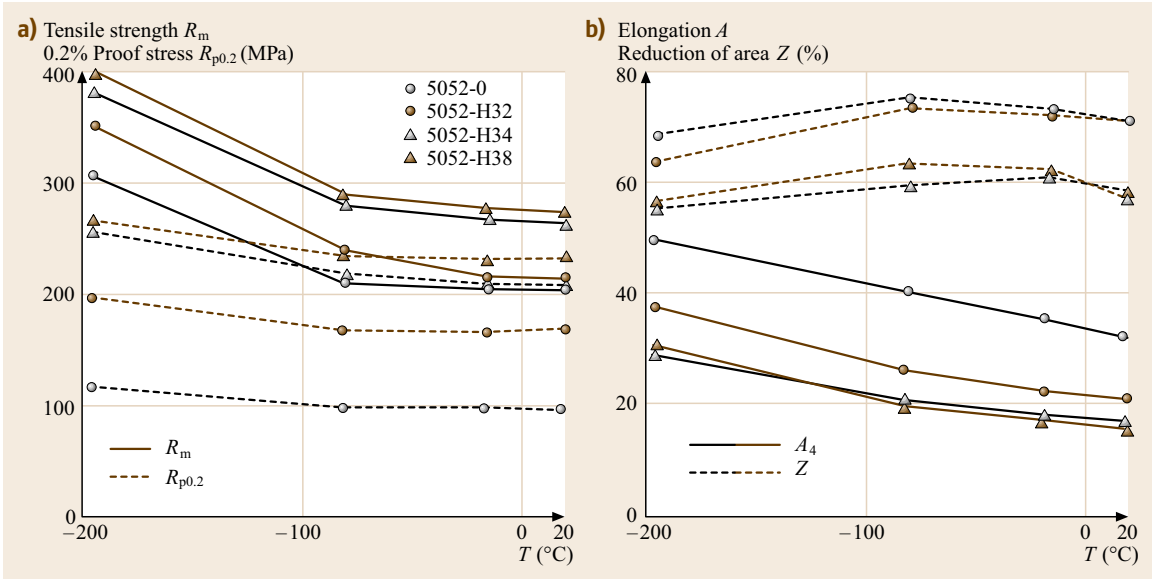


Fig. 6.43a,b Effect of cold working on the tensile properties of EN AW-Al Mg_{2.5} (5052) at low temperatures (after [6.1]). (a) Tensile strength and 0.2 proof stress; (b) elongation and reduction of area

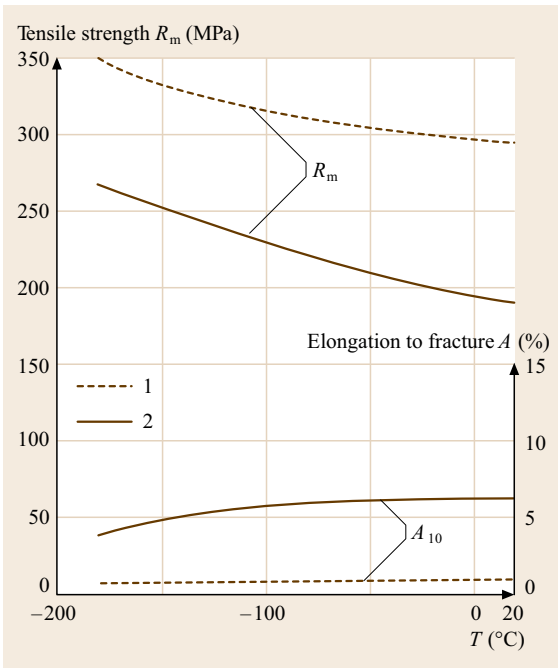


Fig. 6.44 Mechanical properties of artificially aged EN AC-44100 (Al Si12(b)) and EN AC-43000 (Al Si10Mg(a)) casting alloys at low temperatures (after [6.21]). The solid line represents 43000, artificially aged; the dashed line represents 44100, as-cast

age-hardenable alloys and nonage-hardenable alloys. It manifests itself in the shape of the $S-N$ curve

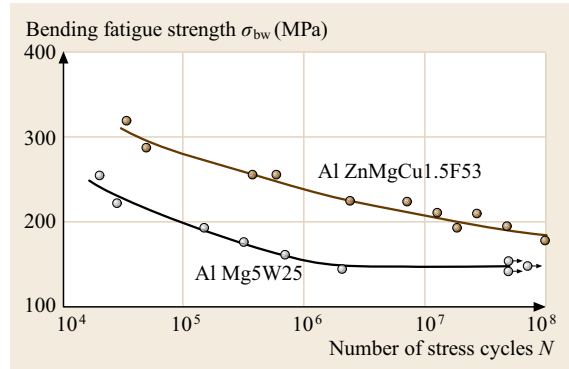


Fig. 6.45 Typical $S-N$ curves for reverse bending tests on an age-hardenable and a nonage-hardenable alloy (after [6.1]), EN AW-7075 (Al Zn5.5MgCu, T651) and EN AW-5019 (Al Mg5, O)

(Fig. 6.45), which is almost horizontal after about 10^6 cycles for nonage-hardenable alloys and after about 10^8 cycles for age-hardenable alloys. Figure 6.45 illustrates that the choice of 10^8 cycles as the ultimate number of stress cycles is regarded as adequate. Figure 6.46 shows fatigue curves for a number of casting alloys.

6.8.2 Technological Properties

Abrasion Resistance

The wear resistance of Al alloys is low, especially in the absence of lubricants. There is no relation between hardness, strength and abrasion resistance. Under suit-

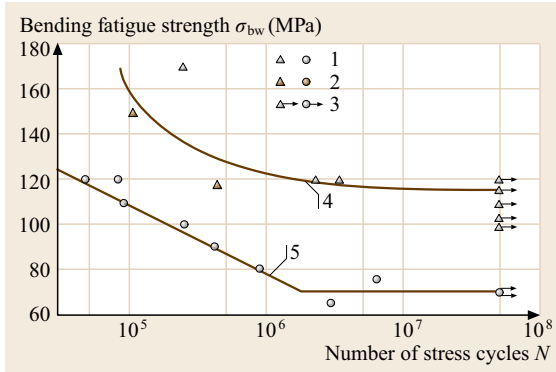


Fig. 6.46 Bending fatigue strength of two aluminum pressure die-casting alloys; flat samples with cast skin (after [6.1]): (1) fracture; (2) fracture, with evidence of defect; (3) no fracture; (4) GD-Al Si6Cu3; (not in EN); (5) EN AC-44300 (Al Si12(Fe))

able conditions of lubrication, aluminum alloys can be safely used where they will encounter friction, as shown by their widespread use in the fabrication of pistons and sliding bearings. Wear can be drastically reduced by the suitable surface treatments.

Sheet Formability

Typical values for deep-drawing indices for commonly used sheet materials are shown in Fig. 6.47, whereas typical values of strain-hardening exponent *n* and degree of anisotropy *r* are given in Table 6.4. The *r* value

Table 6.4 Typical values of strain-hardening exponent *n* and degree of anisotropy *r* for some aluminum-base materials based on data from various sources (after [6.1]); n.a. – not available

| Material | EN AW- | Temper | <i>n</i> | <i>r</i> |
|-------------|--------|--------|----------|----------|
| Al 99.5 | 1050A | O/H111 | 0.25 | 0.62 |
| Al Mn1 | 3103 | O/H111 | 0.15 | n.a. |
| Al Mg3 | 5754 | O/H111 | 0.20 | 0.64 |
| Al Mg3 | 5754 | H14 | 0.16 | 0.75 |
| Al Mg3 | 5754 | H18 | 0.12 | 1.10 |
| Al Mg2Mn0.8 | 5049 | O/H111 | 0.20 | 0.66 |
| Al Mg2Mn0.8 | 5049 | H112 | 0.20 | 0.92 |
| Al Mg4.5Mn | 5063 | O/H111 | 0.15 | n.a. |

is strongly dependent on the manufacturing process in particular, as is the case with all texture-dependent properties. In general, materials with high *n* and *r* values are deep-drawable.

Machinability

There are difficulties involved in classifying aluminum alloys according to their machinability. In general, soft wrought alloys perform worse than other materials regardless of the machining conditions because of chip shape. Harder wrought alloys perform somewhat better and special machining alloys and casting alloys perform best of all. In Si-containing alloys, including wrought alloys, there is a marked increase in tool wear with increasing Si content if the relatively hard Si is present in its elemental form.

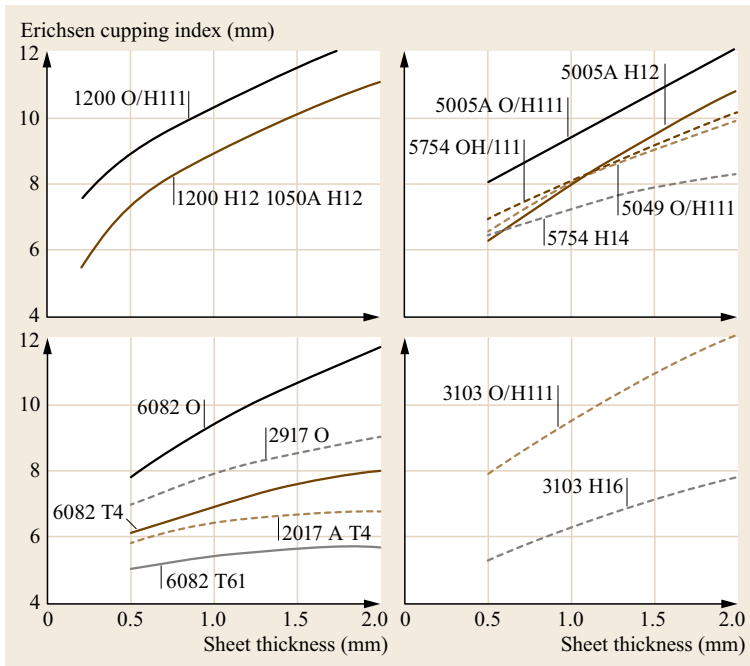


Fig. 6.47 Dependence of deep-drawing index on sheet thickness for different aluminum sheet alloys (after [6.1]). The alloys are: EN AW-1200A (Al 99.0), EN AW-5005A (Al Mg1(C)), EN AW-5754 (Al Mg3), EN AW-5049 (Al Mg2Mn0.8), EN AW-6082 (Al Si1MgMn), EN AW-2017A (Al Cu4MgSi(A)), EN AW-3103 (Al Mn1)

6.8.3 Physical Properties

The most important physical properties of pure Al are listed in Chap. 4, Tables 4.39–4.45. Characteristic ranges of property variations with the amount of impurities or alloying elements are compiled in Table 6.5.

Coefficient of Thermal Expansion

Values of the average linear coefficient of thermal expansion for some Al-based materials at temperatures of practical significance are given in Table 6.6. Alloying leads to only small changes in the coefficient of thermal expansion (Tables 6.5 and 6.6). Si additions with 1.2% reduction in the coefficient of thermal expansion for each wt% Si have the greatest effect of the alloying elements commonly used. This effect is applied to the manufacture of piston alloys.

Specific Heat

The specific heat of aluminum in the solid state increases continuously from 0 at 0 K to a maximum at the melting point. This is only the case with alloys when there are no solid state reactions. The effect of alloying elements in solution is not very marked.

Elastic Properties

The Young's modulus of Al and its alloys is usually taken to be about 70 GPa. Values given in the literature for aluminum of all grades of purity and aluminum alloys range from about 60 to 78 GPa. Unalloyed and low-alloyed materials are found in the lower part of the range. The age-hardenable alloys are in the middle to upper part. The Young's modulus is dependent on texture, because the elastic anisotropy as expressed by the ratio of the elastic moduli for single crystals with [111] and [100] orientations is 1.17. Furthermore, cold working and test temperature have a marked effect (Fig. 6.48).

Electrical Conductivity

The electrical conductivity is influenced largely by alloying or impurities and the structure. Elements present in solid solution lead to a greater reduction in electrical conductivity than precipitates (Figs. 6.4 and 6.5). By use of a suitable combination of heat treatment and cold working, it is possible to obtain microstructures with an adequate combination of tensile strength and electrical conductivity. This is shown in Fig. 6.49, using E-Al MgSi wire as an example.

Behavior in Magnetic Fields

Aluminum is weakly paramagnetic. The specific susceptibility of Al and its alloys is about $7.7 \times 10^{-9} \text{ m}^3 \text{ kg}^{-1}$ at room temperature.

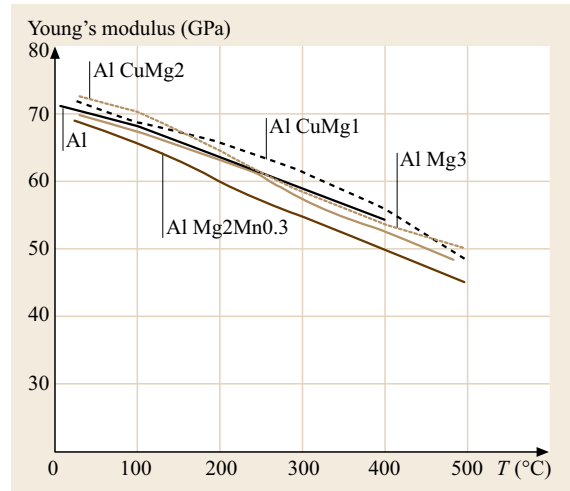


Fig. 6.48 Dependence of Young's modulus E of different Al alloys on temperature; determined using 9 mm thick plate (after [6.25])

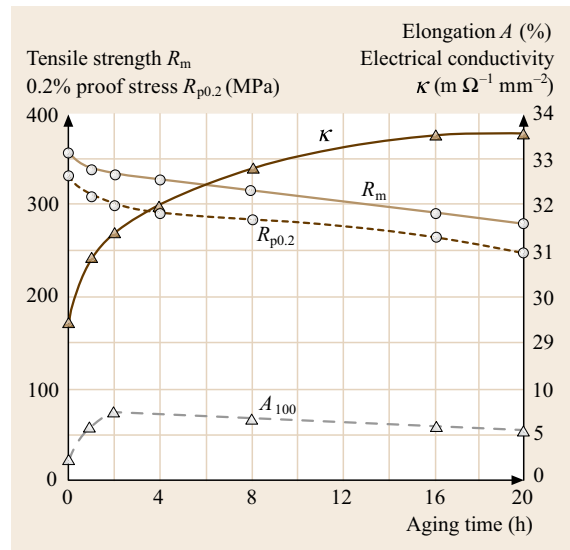


Fig. 6.49 Changes in the mechanical properties and electrical conductivity of electrical-grade E-Al MgSi (≈ 6101) alloy wire during artificial aging at 160°C ; solution treated at 525°C , water quenched, naturally aged for 14 d, 95% cold-worked and then artificially aged (after [6.5])

Nuclear Properties

Thanks to its small absorption cross section for thermal neutrons, aluminum is often used in reactor components requiring low neutron absorption.

Optical Properties

The integral reflection is almost independent of the technical brightening process applied, but it depends on

Table 6.5 Examples of physical properties of aluminum alloys (after [6.1]^a)

| Designation EN AW- | Chemical composition | Density (g cm ⁻³) | Freezing range ^b (°C) | Electrical conductivity (m Ω ⁻¹ mm ⁻²) | Thermal conductivity (W m ⁻¹ K ⁻¹) | Coefficient of linear expansion (10 ⁻⁶ K ⁻¹) |
|-----------------------|-------------------------|----------------------------------|-------------------------------------|---|---|---|
| Wrought alloys | | | | | | |
| 1098 | Al 99.98 | 2.70 | 660 | 37.6 | 232 | 23.6 |
| 1050A | Al 99.5 | 2.70 | 646–657 | 34–36 | 210–220 | 23.5 |
| 1200 | Al 99 | 2.71 | 644–657 | 33–34 | 205–210 | 23.5 |
| 8011A | Al FeSi(A) | 2.71 | 640–655 | 34–35 | 210–220 | 23.5 |
| 3103 | Al Mn1 | 2.73 | 645–655 | 22–28 | 160–200 | 23.5 |
| 3003 | Al Mn1Cu | 2.73 | 643–654 | 23–29 | 160–200 | 23.2 |
| 3105 | Al Mn0.5Mg0.5 | 2.71 | 635–654 | 25–27 | 180–190 | 23.2 |
| 3004 | Al Mn1Mg1 | 2.72 | 629–654 | 23–25 | 160–190 | 23.2 |
| 5005A | Al Mn1(C) | 2.69 | 630–650 | 23–31 | 160–220 | 23.6 |
| 5052 | Al Mg2.5 | 2.68 | 607–649 | 19–21 | 130–150 | 23.8 |
| 5754 | Al Mg3 | 2.66 | 610–640 | 20–23 | 140–160 | 23.9 |
| 5019 | Al Mg5 | 2.64 | 575–630 | 15–19 | 110–140 | 24.1 |
| 5049 | Al Mg2Mn0.8 | 2.71 | 620–650 | 20–25 | 140–180 | 23.7 |
| 5454 | Al Mg2.7Mn | 2.68 | 602–646 | 19–21 | 130–150 | 23.6 |
| 5086 | Al Mg4 | 2.66 | 585–641 | 17–19 | 120–140 | 23.8 |
| 5083 | Al Mg4.5Mn0.7 | 2.66 | 574–638 | 16–19 | 110–140 | 24.2 |
| 6060 | Al MgSi | 2.70 | 585–650 | 28–34 | 200–220 | 23.4 |
| 6181 | Al Si1Mg0.8 | 2.70 | 585–650 | 24–32 | 170–220 | 23.4 |
| 6082 | Al Si1MgMn | 2.70 | 585–650 | 24–32 | 170–220 | 23.4 |
| 6012 | Al MgSiPb | 2.75 | 585–650 | 24–32 | 170–220 | 23.4 |
| 2011 | Al Cu6BiPb | 2.82 | 535–640 | 22–26 | 160–180 | 23.1 |
| 2007 | Al Cu4PbMgMn | 2.85 | 507–650 | 18–22 | 130–160 | 23 |
| 2117 | Al Cu2.5Mg0.5 | 2.74 | 554–650 | 21–25 | 150–180 | 23.8 |
| 2017A | Al Cu4MgSi(A) | 2.80 | 512–650 | 18–28 | 130–200 | 23.0 |
| 2024 | Al Cu4Mg1 | 2.78 | 505–640 | 18–21 | 130–150 | 22.9 |
| 2014 | Al Cu4SiMg | 2.80 | 507–638 | 20–29 | 140–200 | 22.8 |
| 7020 | Al Zn4.5Mg1 | 2.77 | 600–650 | 19–23 | 130–160 | 23.1 |
| 7022 | Al Zn5Mg3Cu | 2.78 | 485–640 | 19–23 | 130–160 | 23.6 |
| 7075 | Al Zn5.5MgCu | 2.80 | 480–640 | 19–23 | 130–160 | 23.4 |
| Casting alloys | | | | | | |
| 44100 | Al Si12(b) | 2.65 | 575–585 | 17–27 | 120–190 | 20 |
| 47000 | Al Si12(Cu) | 2.65 | 570–585 | 16–23 | 110–160 | 20 |
| 43000 | Al Si10Mg(a) | 2.65 | 575–620 | 17–26 | 120–180 | 20 |
| 43200 | Al Si10Mg(Cu) | 2.65 | 570–620 | 16–20 | 110–140 | 20 |
| 42000 | Al Si7Mg | 2.70 | 550–625 | 21–32 | 150–220 | 22 |
| 51000 | Al Mg3(b) | 2.70 | 580–650 | 16–24 | 110–170 | 23 |
| 51300 | Al Mg5 | 2.60 | 560–630 | 15–22 | 100–160 | 23 |
| 51400 | Al Mg5(Si) | 2.60 | 560–630 | 16–21 | 110–150 | 23 |
| 51200 | Al Mg9 | 2.60 | 510–620 | 11–15 | 80–110 | 24 |
| 46200 | Al Si8Cu3 | 2.75 | 510–610 | 14–18 | 100–130 | 22 |
| 45000 | Al Si6Cu4 | 2.75 | 510–620 | 15–18 | 110–130 | 22 |
| 21100 | Al Cu4Ti | 2.75 | 550–640 | 16–20 | 110–140 | 23 |
| 21000 | Al Cu4MgTi | 2.75 | 540–640 | 16–20 | 110–140 | 23 |

^a The actual values will depend on the material composition within the permitted range; electrical and thermal conductivity will also depend on the material structure

^b Where a eutectic structure is expected to form because of segregation, this will solidify at the lowest temperature given

Table 6.6 Linear coefficient of thermal expansion of some Al alloys for different ranges of temperature (after [6.1])

| Designation (according to EN 573.3 and EN 1706) | | Average coefficient of linear expansion (10^{-6} K^{-1}), for the range | | | |
|--|------------|---|-----------|-----------|-----------|
| | | -50–20 °C | 20–100 °C | 20–200 °C | 20–300 °C |
| 1098 | Al 99.98 | 21.8 | 23.6 | 24.5 | 25.5 |
| 1050A | Al 99.5 | 21.7 | 23.5 | 24.4 | 25.4 |
| 3003 | Al Mn1Cu | 21.5 | 23.2 | 24.1 | 25.2 |
| 3004 | Al Mn1Mg1 | 21.5 | 23.2 | 24.1 | 25.1 |
| 5005A | Al Mg1(C) | 21.8 | 23.6 | 24.5 | 25.5 |
| 5019 | Al Mg5 | 22.5 | 24.1 | 25.1 | 26.1 |
| 5474 | Al Mg3Mn | 21.9 | 23.7 | 24.6 | 25.6 |
| 6060 | Al MgSi0.5 | 21.8 | 23.4 | 24.5 | 25.6 |
| 2011 | Al Cu6BiPb | 21.4 | 23.1 | 24.0 | 25.0 |
| 44100 | Al Si12(b) | – | 20.0 | 21.0 | 22.0 |

the purity of the metal. It is 84–85% for high-purity aluminum Al 99.99 and 83–84% for unalloyed aluminum Al 99.9. Higher amounts of diffuse reflection

can be obtained by mechanical or chemical pretreatment, such as sand blasting or strong pickling before brightening.

6.9 Thermal and Mechanical Treatment

Thermal and mechanical treatments have a great influence on the properties of aluminum and its alloys. Moreover, these treatments influence some physical properties, for example the electrical conductivity. Thus, these treatments are used to obtain a material with an optimum of properties required.

6.9.1 Work Hardening

Strengthening by work hardening can be achieved by both cold- and warm working. Figures 6.50–6.52 il-

lustrate the effect of cold working. During hot working, strengthening and softening processes occur simultaneously; with aluminum-based materials, this

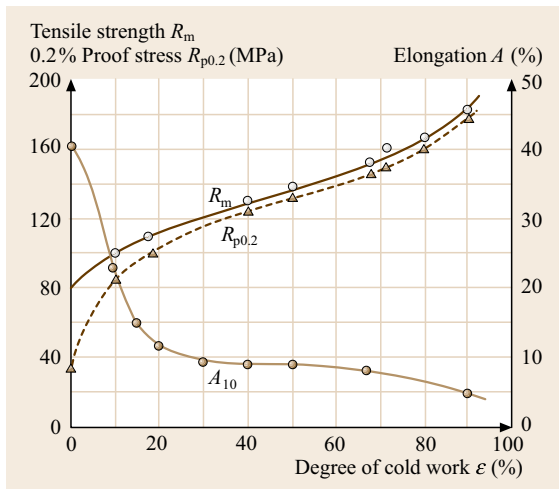


Fig. 6.50 Hardening of EN AW-Al 99.5 strip (0.15 wt% Si, 0.28 wt% Fe) 1050 A, after recrystallization annealing and subsequent cold-rolling (after [6.26])

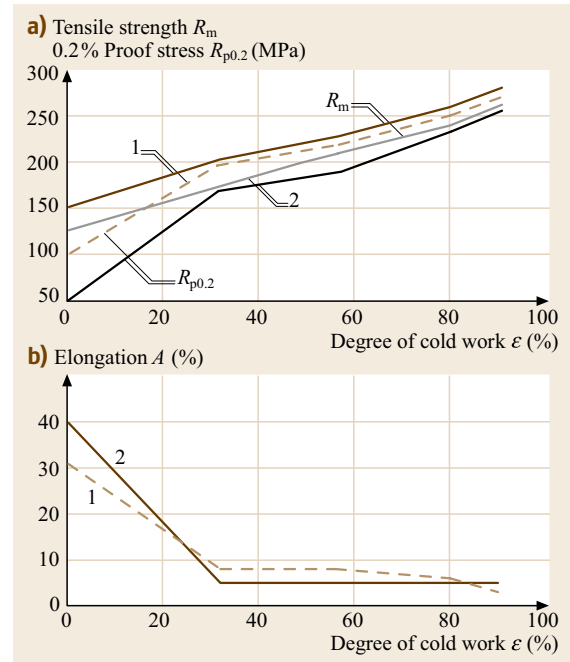


Fig. 6.51a,b Typical mechanical properties ((a) tensile strength and 0.2 proof stress; (b) elongation) of (1) continuously cast and rolled strip and (2) strip produced conventionally by hot-rolling and then cold-rolling cast billets of EN AW-Al Mn1 (3103) (after [6.27])

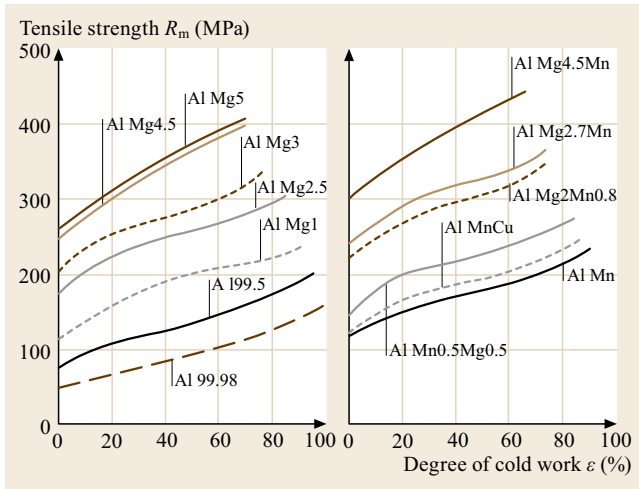


Fig. 6.52 Tensile strength of various wrought nonage-hardenable aluminum alloys (EN AW) as a function of the degree of cold work (after [6.26]): Al Mg4.5 – 5082; Al Mg5 – 5019; Al Mg3 – 5754; Al Mg2.5 – 5052; Al Mg1 – 5005; Al 99.5 – 1050A; Al 99.8 – 1080; Al Mg4.5Mn – 5083; Al Mg2.7Mn – 5454; Al Mg2Mn0.8 – 5049; Al Mn0.5Mg0.5 – 3105; Al Mn – 3103; Al MnCu – 3003

will be above about 150–200 °C. Therefore, hardness decreases with increasing hot-working temperature (Figs. 6.53 and 6.54). The formation of subgrains occurs in the microstructure; their size increases with increasing rolling temperature. Alloying atoms, such as Mg, impede growth or coarsening of the subgrains.

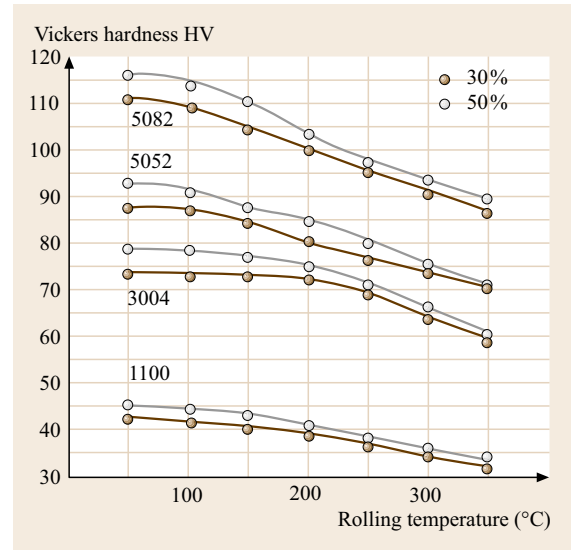


Fig. 6.53 Effect of rolling temperature on hardness; specimens quenched after hot-rolling wrought alloys EN AW: Al 99.0Cu – 1100; Al Mn1Mg2 – 3004; Al Mg2.5 – 5052; Al Mg4.5 – 5082 (after [6.30])

6.9.2 Thermal Softening

Figure 6.54a,b shows typical softening curves for aluminum alloys in three characteristic stages: recovery, recrystallization, and grain growth. In the case of the untreated continuously cast and rolled strip shown in

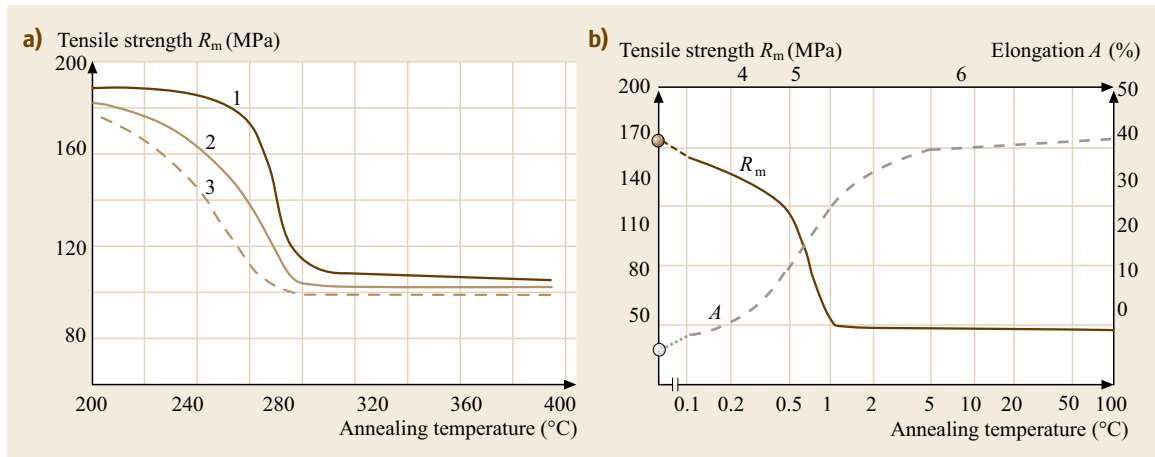


Fig. 6.54a,b Typical softening curves for cold-rolled Al 99.5 (after [6.28, 29]). (a) Recrystallization after different initial tempers to 90% cold work and subsequent annealing for 1 h at different temperatures: (1) continuously cast and rolled strip, subsequently cold-worked without an intermediate annealing treatment; (2) as 1 but with an intermediate annealing treatment for 1 h at 580 °C; (3) strip conventionally produced using permanent mold casting and hot-rolling. (b) Continuously cast and rolled strip, cold-worked 90% and then annealed at 320 °C for time shown; (4) recovery; (5) recrystallization; (6) grain growth

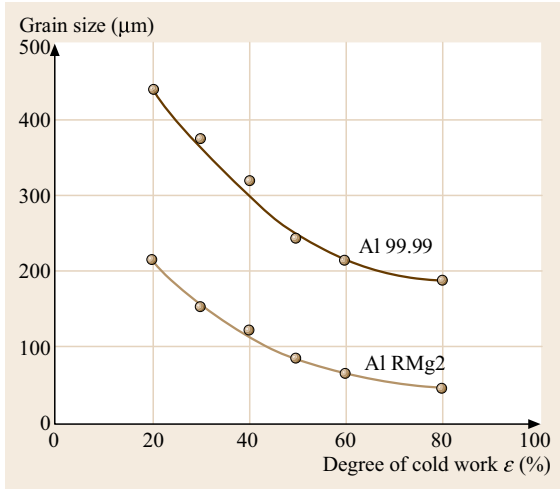


Fig. 6.55 Grain size after complete recrystallization of Al 99.99 and Al RMg2 as a function of degree of cold work (annealed at 350–415 °C until complete recrystallization) (after [6.1])

Fig. 6.54a, recrystallization will occur at temperatures between about 260 and 290 °C. In Fig. 6.54b, recrystallization starts after about half an hour and is complete after about an hour. The softening curves depend not only on the alloy composition but also on the degree of prior cold working to a marked extent. Further factors are the content of alloying and impurity elements, annealing time, heating rate, the microstructure prior to deformation and prior thermomechanical treatment, which can also include the casting process used to produce the starting material. The softening due to recovery or partial recrystallization is very important when producing semifinished products of medium hardness (e.g., half-hard). The relationship between the degree of cold work and grain size is apparent in Fig. 6.55. If the degree of cold work is below a critical value, no recrystallization will occur. This threshold depends on material and prior thermomechanical treatment, and is about 2–15%. If the degree of cold work is near the critical value, coarse grains can form during recrystallization, as clearly shown in the three-dimensional diagram in Fig. 6.56.

Other elements can affect the recrystallization temperature and the grain size after recrystallization. Mg does not have a marked effect (Fig. 6.57), while Mn, Fe, Cr, Ti, V, and Zr increase the recrystallization temperature (Fig. 6.58 delaying effect = plateau). This is dependent on the amount and distribution of these elements, i. e., whether they are present as precipitates or in supersaturated solid solution, and/or whether they form intermetallic phases. In Fig. 6.59 it is clearly apparent that solution treatment reduces the degree of supersaturation

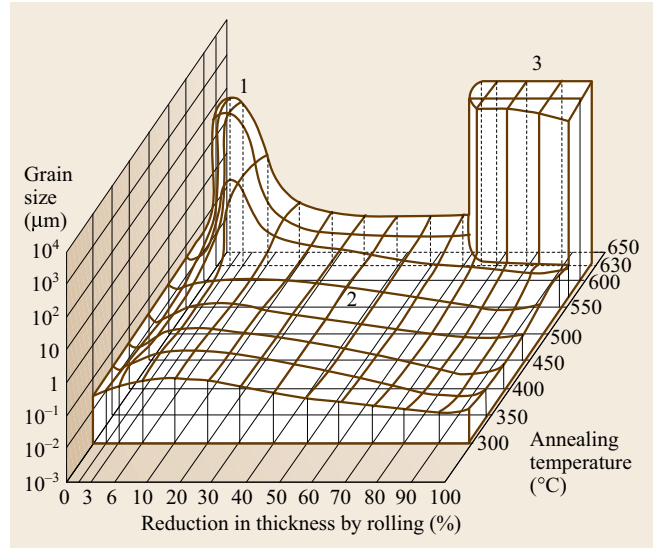


Fig. 6.56 Recrystallization diagram showing grain size of EN AW-Al 99.6 (1060) as a function of cold work and annealing for 2 h at the temperatures shown (after [6.1]): (1) coarse grains in the region of critical degree of cold work (primary recrystallization); (2) area of primary recrystallization with fine and medium-sized grains; (3) coarse grains as a result of secondary recrystallization

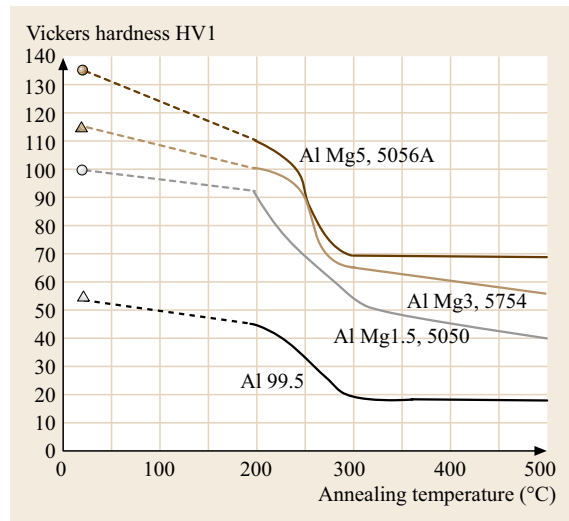


Fig. 6.57 Effect of Al-Mg alloy composition (wrought and alloy EN AW-) on the softening behavior; the material was 90% cold-worked and annealed for 1 h at the temperature shown (after [6.29])

and that the range over which tensile strength and 0.2% proof stress decrease rapidly with temperature is thus shifted to significantly lower temperatures. Interactions between the various elements present can also affect recrystallization behavior.

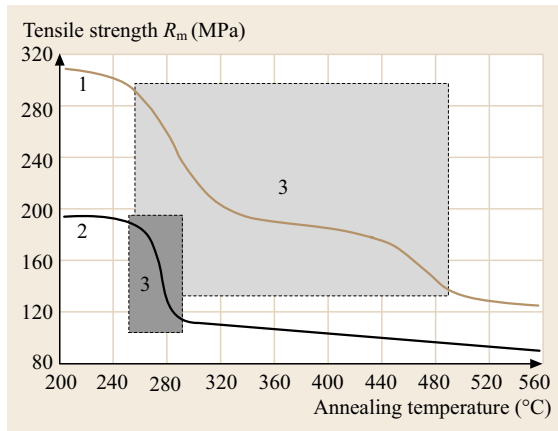


Fig. 6.58 Comparison of softening curves for cast and hot-rolled Al 99.5 and AlMn1 strip; material cold-worked 90% and annealed for 1 h at the temperature shown (after [6.29]): (1) cast and hot-rolled AlMn1 (3103) strip; (2) cast and hot-rolled Al 99.5 (1050A) strip; (3) recrystallization range

6.9.3 Soft Annealing, Stabilization

With cold-worked materials, soft annealing consists of recrystallization annealing. The duration of the treatment, degree of cold work, and intermediate annealing treatments need to be selected with grain size in mind. In age-hardenable alloys, soft annealing permits most of the supersaturated components to precipitate out in coarse form or coherent or partially coherent phases to transform to incoherent stable phases. Soft annealing of casting alloys involves annealing the as-cast structure at 350–450 °C. With age-hardenable alloys, this is also possible using a solution treatment followed by furnace cooling or nonforced air cooling. Al-Mg alloys

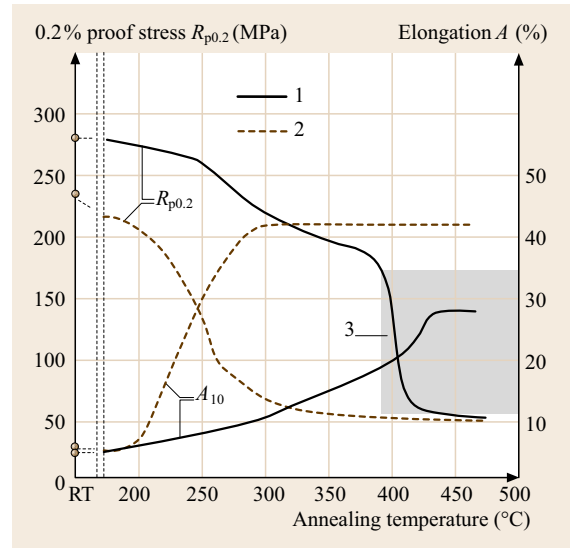


Fig. 6.59 Softening curves for continuously cast and rolled EN AW-Al Mn1 (3103) strip after annealing for 4 h at elevated temperatures (after [6.31, 32]): (1) untreated material, as-cast condition; (2) homogenized at 540 °C after cold working; (3) coarse grains

with more than 4 wt% Mg may have to be stabilized to produce a structure that is not susceptible to intergranular corrosion.

6.9.4 Stress-Relieving

The temperatures used for thermal stress relief are relatively low, i. e., at the lower end of the recovery range, or even lower, and between 200 and 300 °C for nonage-hardenable alloy castings, otherwise there will be an unacceptably large loss of strength.

Table 6.7 Conditions for aging treatments^a

| Alloy | Annealing temperature ^b (°C) | Quenching medium | Natural aging time (d) | Artificial aging Temperature (°C) | Time (h) |
|---------------|---|-------------------|------------------------|--------------------------------------|----------------------------------|
| E-Al MgSi | 525–540 | Water | 5–8 | 155–190 | 4–16 |
| Al MgSi0.5 | 525–540 | Air/water | 5–8 | 155–190 | 4–16 |
| Al MgSi1 | 525–540 | Water/air | 5–8 | 155–190 | 4–16 |
| Al Mg1SiCu | 525–540 | Water/air | 5–8 | 155–190 | 4–16 |
| Al CuBiPb | 515–525 | Water up to 65 °C | 5–8 | 165–185 | 8–16 |
| Al Cu4MgSi(A) | 495–505 | Water | 5–8 | ^c | ^c |
| Al Cu4Mg1 | 495–505 | Water | 5–8 | 180–195 ^c | 16–24 ^c |
| Al Zn4.5Mg | 460–485 | Air at least | min. 90 | I 90–100/ II 140–160 ^d | I 8–12/ II 16–24 ^d |

^a Recommendations only; exact specification as per agreement with semifinishing plant

^b Metal temperature

^c Usually only naturally aged

^d Stages I and II of step annealing

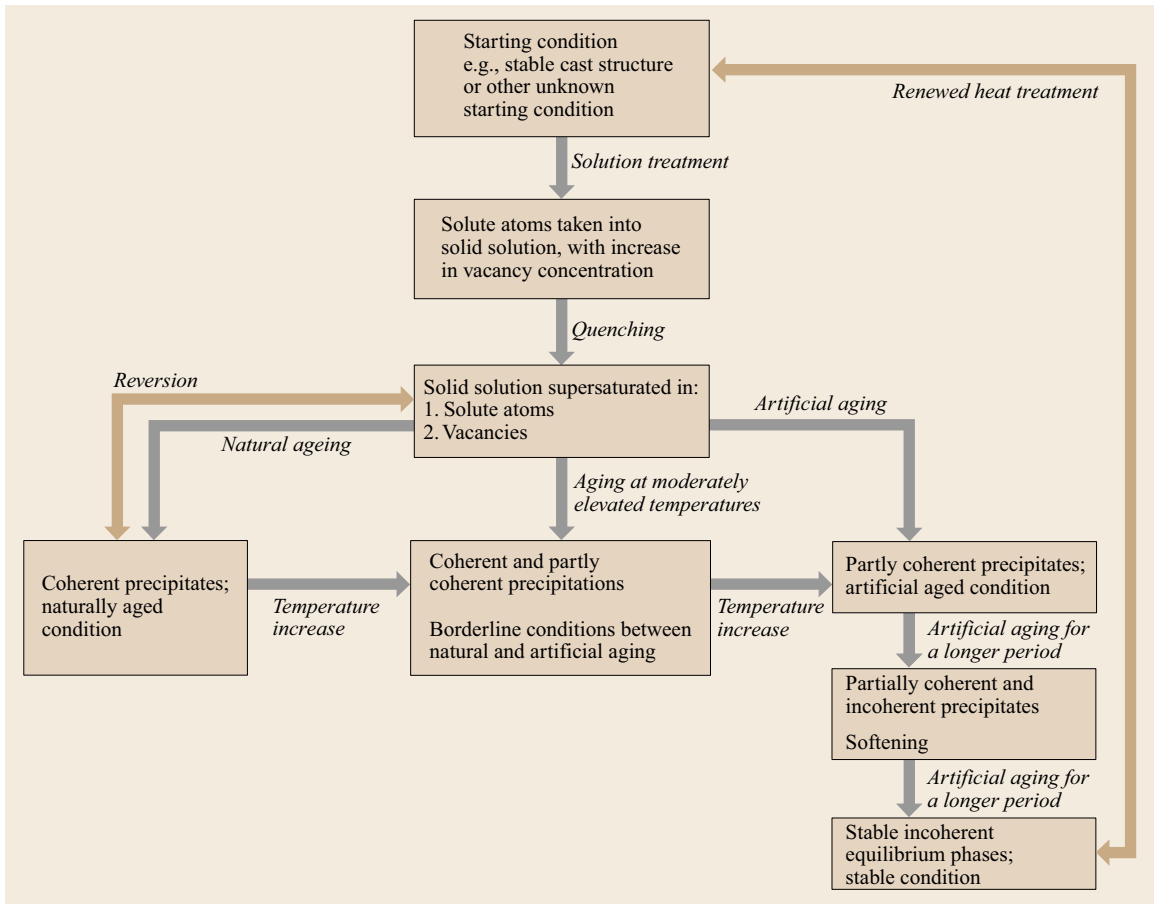


Fig. 6.60 Schematic of the age-hardening process

6.9.5 Homogenization

This treatment is used for the elimination of residual casting stresses and segregation, for dissolution of eutectoid components at grain boundaries, or to produce a more uniform precipitation of supersaturated elements (e.g., Mn and Fe). Additionally, the elements that are responsible for hardening in age-hardenable alloys are taken into solid solution. A homogenization is carried out at temperatures that are composition-dependent and close to the solidus temperature of the alloy in question. Long exposure times are required, typically about 10–12 h but possibly even longer, depending on the relevant diffusion coefficients and microstructure.

6.9.6 Aging

Age hardening treatments require the three steps of solution treatment, quenching, and aging (Fig. 6.60). The purpose of solution treatment is to produce a homoge-

nous α -Al solid solution. The annealing temperature is determined by the relevant phase. It should be as high as possible in order to avoid excessively long annealing times, but lower than the solidus of α and the melting point of the lowest melting phase (Table 6.7). It should be noted that segregation effects tend to displace the effective phase boundaries to lower temperatures and incipient melting may occur. In addition, the effect of the selected solution treatment temperature on strength levels attained after aging will vary with alloy (Figs. 6.61 and 6.62). The annealing time depends mainly on the initial condition of the semifinished material, type of semifinished product, and the wall thickness (Figs. 6.63 and 6.64).

During quenching, it is important to pass through the temperature range around 200 °C as quickly as possible, in order to prevent premature precipitation of the elements in supersaturated solid solution.

Some alloys require high cooling rates, such as those obtained by quenching in water. For others, especially with thinner sections, cooling in a forced draft

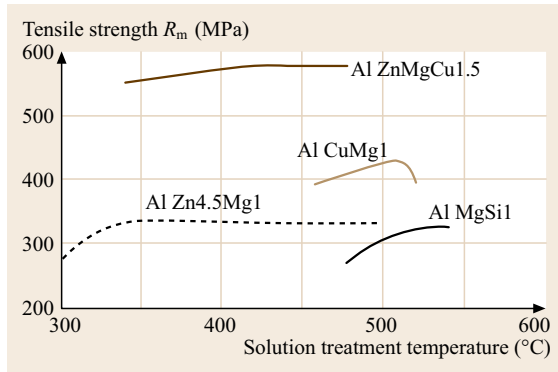


Fig. 6.61 Effect of solution treatment temperature on the tensile strength of wrought aluminum alloys (after [6.1]): EN AW-7075, Al Zn5.5MgCu, 24 h at 120 °C; EN AW-2017A, Al Cu4MgSi(A), 5 d at room temperature; EN AW-7020, (Al Zn4.5Mg1), 1 month at room temperature; EN AW-6082, Al Si1MgMn, 16 h at 160 °C

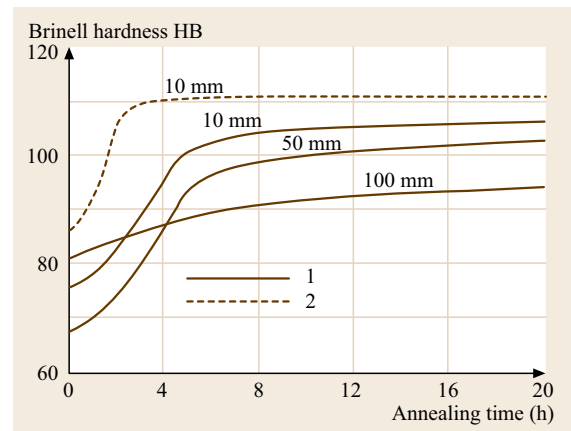


Fig. 6.63 Effect of annealing time on the hardness of artificially aged EN AC-Al Si10Mg(a) (43000) casting alloy for different casting techniques and specimen diameters (after [6.1]): (1) sand cast; (2) permanent mold cast

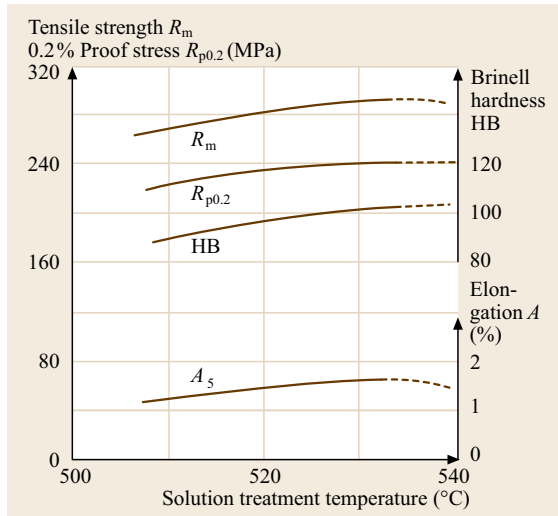


Fig. 6.62 Effect of solution treatment temperature on the mechanical properties of EN AC-Al Si10Mg(a) (43000) casting alloy after subsequent aging (after [6.1])

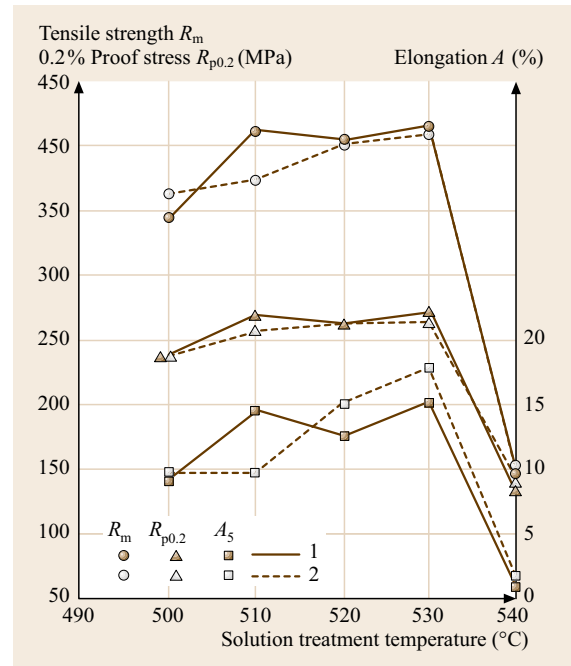


Fig. 6.64 Dependence of mechanical properties of naturally aged EN AC-Al Cu4TiMgF (21000) casting alloy on the maximum solution treatment temperature: (1) step annealing; (2) single-step annealing

of air or a mist spray suffices. In this case, quenching takes place immediately after hot working or even directly in the extrusion press. With most alloys it is important that the annealed material is rapidly transferred to the quenching bath as any delay (incipient cooling) can have a detrimental effect on strength and corrosion resistance.

After the first two stages of the hardening process, the solid solution will be supersaturated in both vacancies and solute atoms. It will tend to attain equilibrium conditions by precipitation of the supersaturated solute atoms. As the process is both temperature- and time-

dependent, precipitation is basically possible either by natural or artificial aging, i. e., at room or elevated temperature, respectively.

Aging at room temperature, or slightly elevated temperature, is accompanied by the formation of metastable GP zones. These metastable phases in-

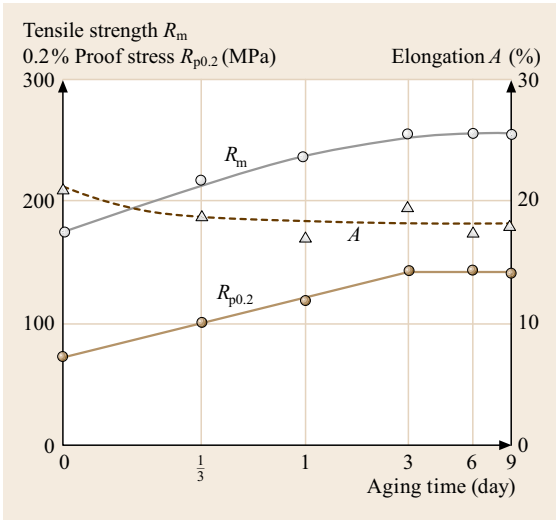


Fig. 6.65 Natural aging of EN AW-6082, Al Si1MgMn alloy (after [6.33])

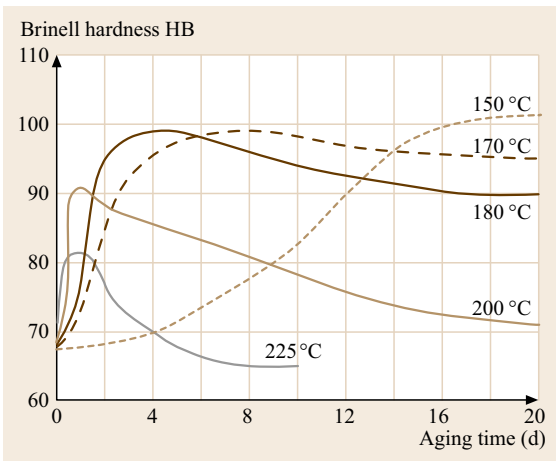


Fig. 6.66 Artificial aging of EN AC-Al Si10Mg (43000) casting alloy (after [6.1])

crease the strength by differing amounts depending on their type, size, volume fraction, and distribution. With fully coherent precipitates, the crystal lattice is strongly strained locally, resulting in a marked increase in hardness and strength, while ductility and electrical conductivity decreases (Figs. 6.65 and 6.66).

At higher aging temperatures of about 100–200 °C, metastable phases form that are partially coherent. The local coherency strain is less pronounced because the stresses are partly reduced by the formation of interfacial dislocations. This would lead to a lower increase in strength in principle. However, since the particle size of the metastable phases formed in this range is often

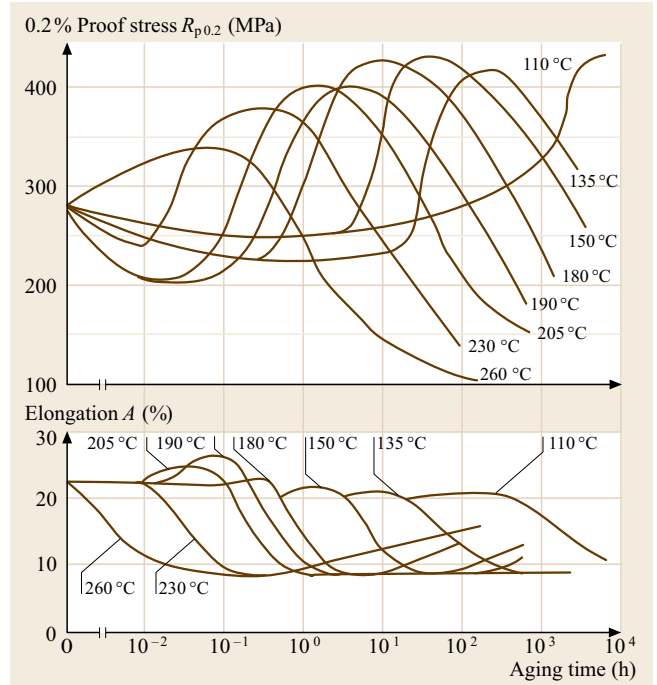


Fig. 6.67 Artificial aging curves for EN AW-2014, Al CuSiMg alloy (after [6.1])

larger than that of the coherent phases that result from natural aging, there is a marked increase in strength (Figs. 6.67 and 6.68).

Higher temperatures and longer aging times lead to the formation of incoherent equilibrium phases (e.g., Al_2Cu , Mg_2Si , and MgZn_2) and there is a reduction in the hardening effect. This is called overaging.

6.9.7 Effects of Plastic Deformation on Age-Hardening Behavior

For wrought age-hardenable aluminum alloys, the combination of heat treatments with hot and/or cold working (thermomechanical treatment) is of great practical significance. This method can be used to obtain a better combination of mechanical properties, such as moderate ductility and higher strength. The effects of thermomechanical treatments can be attributed to the fact that all processes occurring during heat treatment are influenced by the concentration of defects introduced during working. It is not necessary to carry out both steps simultaneously; the heat treatment can be carried out after forming [6.34]. As far as precipitation is concerned, lattice defects facilitate diffusion and at the same time act as nucleation sites. Thus, by deforming a material by a certain amount *prior* to aging and thereby obtaining the desired defect concentration, one can influence the

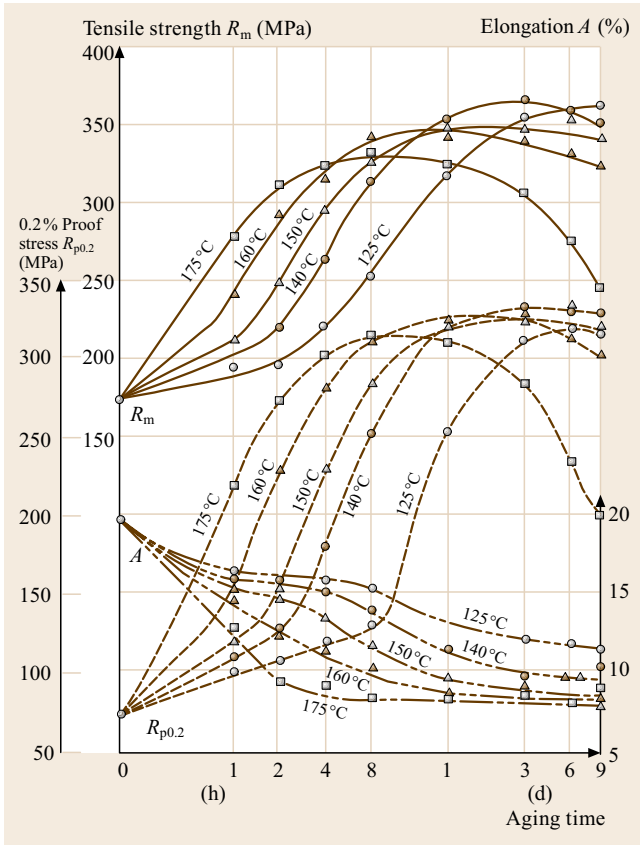


Fig. 6.68 Artificial aging curves for EN AW-6082, Al Si1MgMn alloy after solution treatment at 520 °C and water quenching

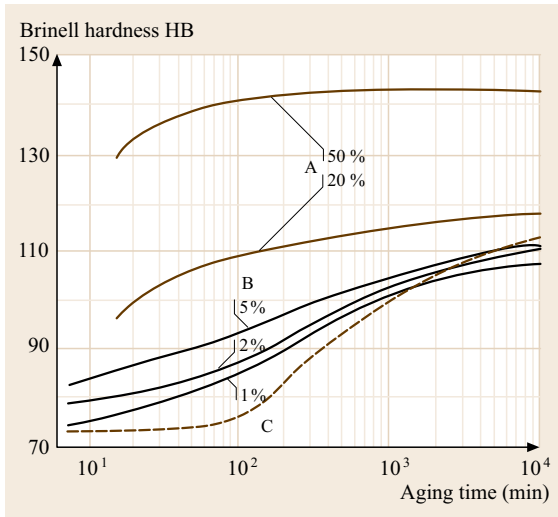


Fig. 6.69 Effect of cold work on the natural aging of EN AW-2017A Al Cu4MgSi(A) (after [6.1]); A – rolled; B – stretched; C – without cold work

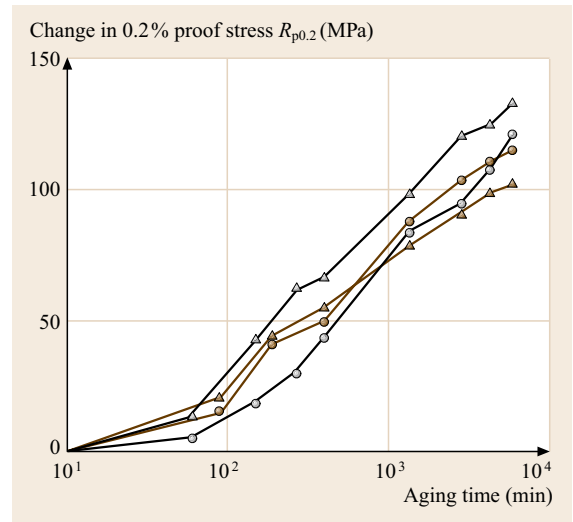


Fig. 6.70 Changes in the 0.2% proof stress during natural aging of 0.5 mm diameter wire specimens (EN AW-7022, Al Zn5Mg3Cu) alloys after different degrees of cold working. The alloys were first solution-treated at 490 °C and then immediately subjected to cold working as indicated in the text (after [6.35])

size, quantity, and distribution of the precipitates that form subsequently. It is important, however, that the final aging treatment is carried out at a temperature below the recrystallization temperature, as the lattice defect concentration that is generated is fully effective only then.

Controlled hot working, often in combination with additional heat treatments, is another form of thermo-mechanical treatment and is used to improve fracture toughness, creep strength, and fatigue strength. One tries to obtain a suitable recrystallized grain size and an optimum distribution of lattice defects and precipitates. Such treatments are very often used with high strength Al-Zn-Mg-Cu alloys. They usually consist of a series of solution treatments with controlled cooling and hot-rolling under well-defined conditions. Cold working carried out between the various stages of a step-aging treatment is also referred to as thermomechanical treatment. Examples are shown in Figs. 6.69 and 6.70.

6.9.8 Simultaneous Softening and Precipitation

One of the factors that influence the softening of an alloy is the possible supersaturation by alloying of impurity elements. Supersaturation can be achieved deliberately, e.g., by solution treatment and subsequent quenching, or, as is often the case, it may be the result

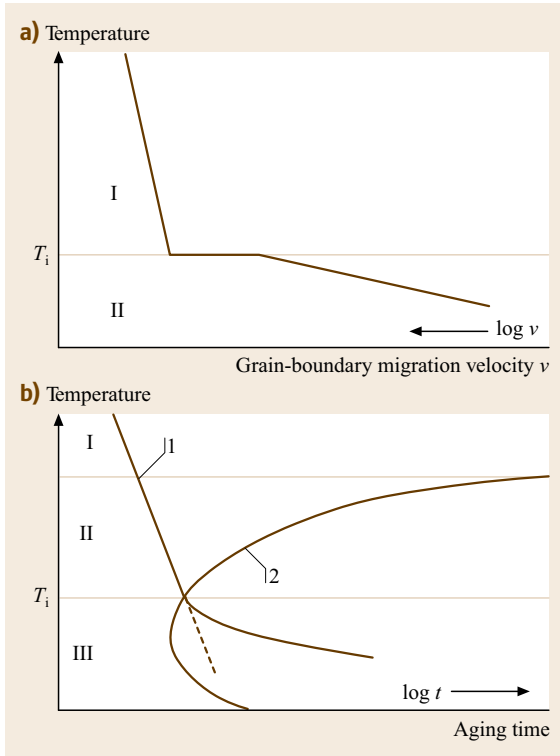


Fig. 6.71a,b Effect of segregation and precipitation on recrystallization (grain-boundary migration): (1) start of recrystallization; (2) start of precipitation. **(a)** Basic effects of solute atom clusters on the grain boundary migration velocity (after [6.36]). Region I, high temperatures: The grain boundary migration velocity is only weakly dependent on temperature because it is unaffected by the clustering (\rightarrow high velocity). Region II: Below T_i , the mobility of the boundaries is reduced because atom clusters have to be dragged along by the boundary, and the diffusion rate of these atoms determines the migration velocity of the boundary (\rightarrow low velocity). **(b)** Inter-relationship between recrystallization and precipitation as a TTT (time-temperature-transformation) diagram (after [6.37]). Region I: Recrystallization as a homogenous stable solid solution, unaffected by precipitation processes, i. e., at these temperatures there is no longer any supersaturation. Region II: Recrystallization in a supersaturated solid solution; the number of potential precipitation nuclei (dislocations) decreases. Result: Fewer but larger precipitations. Region III: Precipitation prior to recrystallization, or simultaneously (T_i). Result: the precipitates delay recrystallization significantly

Fig. 6.74 TTT diagram for Al-0.5 wt% Fe-0.15 wt% Si alloy Harvey cast strip after 80% cold work (after [6.38]). (1) start of precipitation; (2) recrystallization zone \blacktriangleright

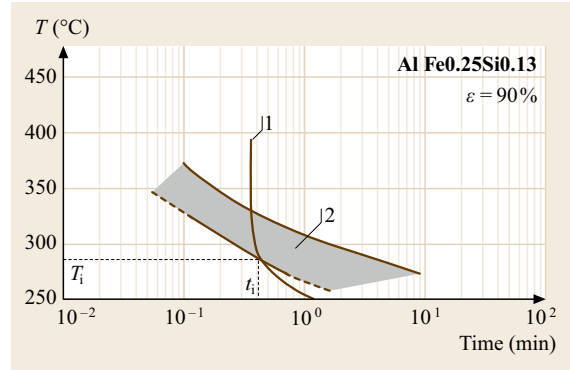


Fig. 6.72 TTT diagram for Al-0.25 wt% Fe-0.13 wt% Si alloy Hunter-Engineering cast strip after 90% cold work (after [6.28]): (1) first signs of precipitation; (2) recrystallization zone

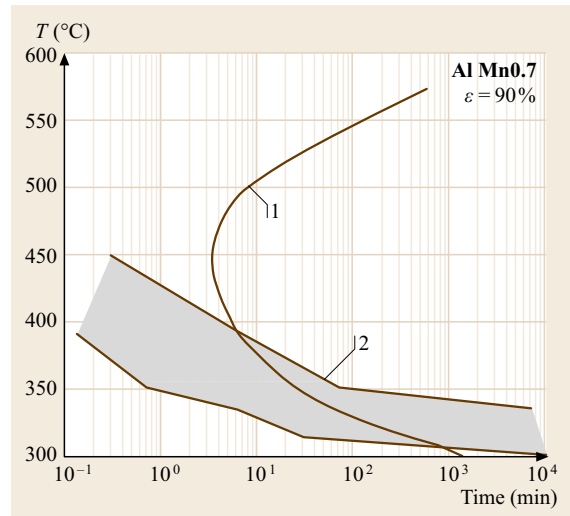
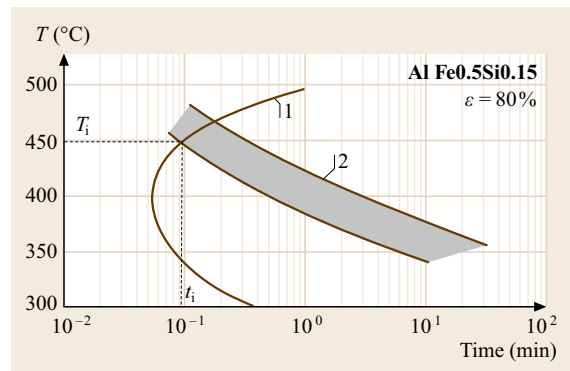


Fig. 6.73 TTT diagram showing precipitation and recrystallization in 90% cold-rolled, high-purity Al Mn0.7 alloy, strip produced by permanent mold casting, hot-rolling, and then cold-rolling (after [6.39]): (1) start of precipitation; (2) recrystallization zone



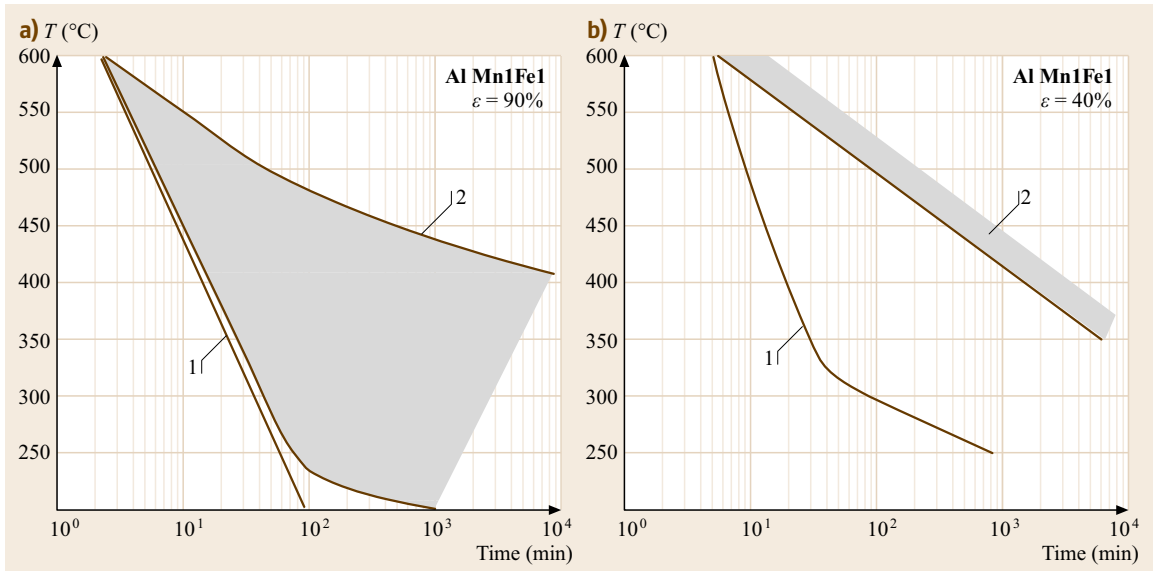


Fig. 6.75a,b TTT diagrams for precipitation and recrystallization in commercially pure Al Mn1Fe1 (0.16 wt% Si), Hunter-Engineering cast strip after varying degrees of cold-rolling (**(a)** 90%, **(b)** 40%) (after [6.40]): (1) start of precipitation; (2) recrystallization zone

of rapid cooling, e.g., of castings. If such a supersaturated material is cold-worked and then aged, it reveals markedly different softening behavior because solute atom clusters or precipitates are formed during recovery at lattice defects in the deformed or recovered structure which pin lattice defects and the formation of solute atom clusters or of precipitates during recrystallization at the recrystallization front, which pin down the recrystallization front. There is a slowing down of the softening process as a result of these pinning effects (Fig. 6.71a,b).

The Stage III area in Fig. 6.71b is of particular interest, as by definition this is a thermomechanical treatment because the lattice defects introduced by working are fully effective during the formation of the precipitates. Dislocations, which are present in large quantities, act as nuclei for precipitation and this results in the formation of numerous finely dispersed precipitates. These impair subsequent recrystallization at every stage – the formation of recrystallization nuclei, the moving of boundaries, and the subsequent grain growth. These effects increase the thermal resistance and delay the loss of strength that occurs after prolonged exposure because of grain growth. Figures 6.72–6.76 show some

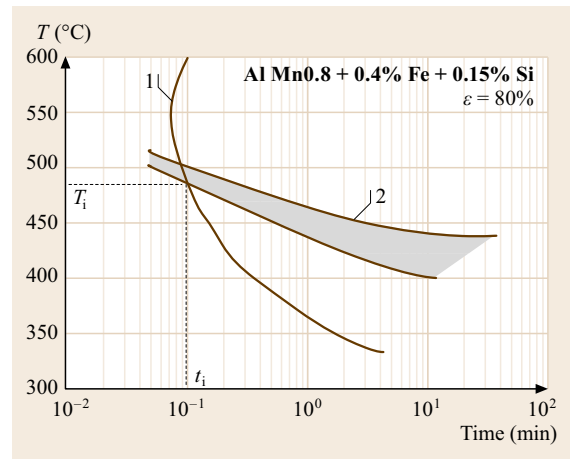


Fig. 6.76a,b TTT diagram showing precipitation and recrystallization in commercially pure Al Mn0.8 alloy strip (0.4 wt% Fe and 0.15 wt% Si) produced by strip casting and 85% cold-rolled (after [6.41–43]): (1) start of precipitation; (2) recrystallization zone

examples of TTT-diagrams for unalloyed aluminum and for alloys.

6.10 Corrosion Behavior of Aluminum

From a thermodynamic point of view, aluminum would have to react with water to form hydrogen. However, Al and Al alloys have proven to be very corrosion-resistant in a wide range of practical applications. This corrosion resistance is attributable to the reaction of Al with oxygen or water vapor and the formation of a thin but compact natural oxide film when it is exposed to air, i. e., Al is passivated. In contrast to the oxide layers formed on many other materials, this oxide layer is strongly adherent and thus protects the underlying metal against further oxidation. This property explains the good resistance of aluminum when exposed to the weather or a large number of organic and inorganic substances. The corrosion resistance can be increased further by various surface treatments.

Aluminum and all standardized aluminum alloys are nontoxic. Aluminum products are easy to clean, can be sterilized and meet all hygienic and antitoxic requirements.

6.10.1 Surface Layers

Aluminum and Al alloys react with oxygen and water vapor in the air to produce a thin, compact surface oxide film that protects the underlying metal from further attack (Fig. 6.77). The surface layer contains mainly amorphous Al_2O_3 in several layers. The so-called barrier layer has an extremely low conductivity for electrons and ions and thus acts as an insulator in any interfacial electrochemical reactions. It thus affords effective protection against corrosion. If mechanical damage of the protective layer occurs, or if the layer is removed by pickling, it re-forms immediately. Aluminum and Al alloys thus exhibit good corrosion resistance to chemicals, seawater, and the weather.

The oxide film that forms on bare aluminum in dry air at room temperature grows to a thickness of a few

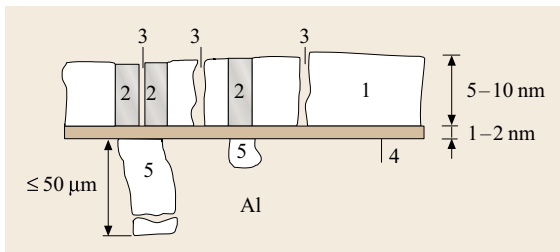


Fig. 6.77 Schematic representation of the structure of the oxide film formed on unalloyed aluminum in dry air; the total thickness is typically 0.005–0.02 mm (after [6.44]). Al = aluminum; 1 = surface layer; 2 = mixed oxides; 3 = pores; 4 = barrier layer; 5 = heterogeneous components

μm in a few minutes. It then grows to about two or three times this thickness in a few days at a continuously decreasing rate, so-called self-protection. Higher temperatures, such as those during heat treatments, accelerate the rate of growth of the natural oxide layer and lead to the growth of thicker films (Fig. 6.78). In moist air, the oxide films grow rapidly at first but then more slowly, and they are markedly thicker than the films formed in dry air.

The composition of the atmosphere has a significant effect on the behavior of the oxide layer. The aggressiveness of the atmosphere is particularly dependent on the amounts of sulfur dioxide, sulfur trioxide, dust, soot, and salts present. Rain water hitting the surface and running off flushes away these substances and thus reduces their influence.

Tap water or natural waters cause growth of the outer layer on top of the barrier layer of the oxide. The growth will depend on the alloy composition, the nature of the water, and temperature. In aggressive waters, especially those containing chlorides and heavy metals, pitting corrosion can occur if oxygen from the air or other oxidizing media are introduced into the water. Traces of Cu (from copper piping or fittings containing copper) are particularly aggressive. Copper ions enter the oxide layer on the aluminum surface via defects

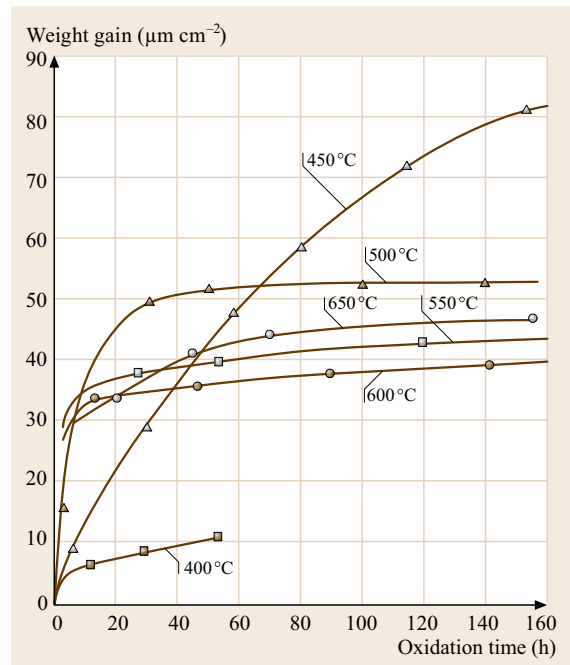


Fig. 6.78 Growth of the oxide film on superpurity aluminum in dry oxygen during the first 160 h (after [6.15])

and precipitate out as metallic Cu. Copper then acts as a cathode in the resulting local galvanic element such that Al is dissolved anodically.

6.10.2 Corrosion

If Al is exposed to acids or bases these dissolve the oxide film. The pH value of the electrolyte strongly influences corrosion in aqueous media. The protective film on aluminum is practically insoluble in the pH range from of 4.5–8.5, which explains why aluminum is usually only used in this range.

Aluminum alloys have heterogeneous microstructural components such as intermetallic phases and resulting oxides in the surface and barrier layers. This explains why unalloyed aluminum and aluminum alloys have lower corrosion resistance than high-purity aluminum.

Apart from the effects of alloying and impurities, there are some other factors affecting corrosion, for example, changes in microstructure by thermal or mechanical treatments and ensuing changes of the surface condition.

Corrosion protection covers any measure aimed at modifying a corrosion system in order to mitigate corrosion damage. This can involve influencing the properties of the metal or the corrosive medium, or separating the metal from the medium by the use of protective layers. One can differentiate between active and passive measures. Passive measures, such as the use of organic polymer coatings (paints), will provide temporary protection, the level of which will depend on the nature, thickness, and quality of the layer. Active measures, such as the use of sacrificial magnesium or zinc anodes, offer long-term protection.

References

- 6.1 C. Kammer: *Aluminium Handbook 1, Fundamentals and Materials* (Beuth-Verlag, Berlin 2012)
- 6.2 U.S. Geological Survey: *Mineral Commodity Summaries 2017* (USGS, Reston 2017), <https://doi.org/10.3133/70180197>
- 6.3 H.W.L. Phillips: *Equilibrium Diagrams of Aluminium Alloy System* (The Aluminium Development Association, London 1961)
- 6.4 J. Thonstad, P. Fellner, G.M. Haarberg, J. Hives, H. Kvande, A. Sterten: *Aluminium Electrolysis – Fundamentals of the Hall-Héroult Process*, 3rd edn. (Aluminium Verlag, Düsseldorf 2001)
- 6.5 E. Nachtigall, H. Landerl: The treatment of the conductor alloy E-AlMgSi, *Alum. Ranshofen Mitt.* **2**, 40–43 (1955), in German
- 6.6 E. Nachtigall, G. Lang: Electrical conductivity of aluminium castings, *Mitt. Ver. Metall. Ranshofen-Berndorf*, 16–19 (1965), in German
- 6.7 C.H. Hamann, W. Vielstich: *Elektrochemie*, 4th edn. (Wiley-VCH, Weinheim 2005), in German
- 6.8 L.F. Mondolfo: *Aluminium Alloys – Structure and Properties* (Butterworths, London 1976)
- 6.9 H. Schumann, H. Oettel: *Metallografie*, 15th edn. (Wiley-VCH, Weinheim 2005), in German
- 6.10 E. Schürmann, I.K. Geissler: Solid-state phase equilibria in the Al and Mg rich areas of the Al–Mg–Li system, *Giessereiforschung* **32**, 163–174 (1981), in German
- 6.11 C. Kammer: *Thermomechanical treatment of Al strip casting*, Ph.D. Thesis (TU Bergakademie Freiberg, Freiberg 1989), in German
- 6.12 A. Dons: AlFeSi-Particles in industrially cast aluminium alloys, *Z. Metall.* **76**, 609–612 (1985)
- 6.13 A. Cziraki, B. Fogarassy, I. Szábo: Structure of high purity Al–Fe–Si-cast with different cooling rates, *Cryst. Res. Technol.* Berlin **20**, 279–281 (1985)
- 6.14 H. Westengen: Structure inhomogenities in direct chill cast sheet ingots of commercial pure aluminium, *Z. Metall.* **73**, 360–368 (1982)
- 6.15 H.P. Godard, W.B. Jepson, M.R. Bothwell, R.L. Kane: *The Corrosion of Light Metals* (Wiley, New York 1967)
- 6.16 K.R. Van Horn: *Aluminium. Vol. 1: Properties, Physical Metallurgy and Phase Diagrams* (ASM, Metals Park 1967)
- 6.17 D. Altenpohl: *Aluminium and Aluminium-Alloys* (Springer, Berlin, Heidelberg 1965), in German
- 6.18 U. Hielscher, H. Arbenz, H. Diekmann: Properties of AlSi-casting alloys with low iron content, *Giesserei* **53**, 125–133 (1966), in German
- 6.19 U. Hielscher: Ductile aluminium–silicon casting alloys for safety components in cars, *Schweiz. Alum. Rundsch.* **29**, 13–15 (1979), in German
- 6.20 U. Hielscher, R. Klos: A new low iron diecasting alloy, *Aluminium* **71**, 676–685 (1995), in German
- 6.21 W. Jung-König, U. Zwicker: Behaviour of light metal alloys on heating, *Aluminium* **34**, 337–345 (1958), in German
- 6.22 H. Vosskühler: Aluminium-Gusslegierungen hoher Dauerstandfestigkeit mit Magnesium und Silicium, *Aluminium* **31**, 219–222 (1955)
- 6.23 K. Wellinger, E. Keil, G. Maier: Strength of aluminium and its alloys up to 300 °C, *Aluminium* **34**, 458–463 (1958), in German
- 6.24 K. Wellinger, E. Keil: On the mechanical properties of aluminium and aluminium alloys at elevated temperatures, *Aluminium* **39**, 372–377 (1963), in German
- 6.25 E. Richter, E. Hanitzsch: Elastic modulus and other physical properties of aluminium–base materials. Part 1, *Aluminium* **70**, 570–574 (1994), in German
- 6.26 D. Lenz, G.M. Renouard: Definition of cold rolled tempers by means of flow curves and energy of

- deformation, *Aluminium* **46**, 694–699 (1970), in German
- 6.27 A. Odok, G. Thym: The technical and economic advantages of continuous strip casting, *Aluminium Engl. Suppl.* **50**, E9–E11 (1974), English translation
- 6.28 C. Kammer, M. Krumnacker: Thermomechanical treatment of continuously cast and rolled Al99.5 alloy, *Neue Hütte* **35**, 418–421 (1990), in German
- 6.29 C. Kammer, M. Krumnacker: Comparison of the strengthening effects in strip cast Al99.5, AlMn1 and AlMn1Fe1, *Metall* **45**, 135–138 (1991), in German
- 6.30 T. Doko, Y. Inabayashi, C. Fujikura: Structural variation during hot rolling at lower temperature of aluminum alloys, *J. Jpn. Inst. Light Met.* **41**(12), 853–857 (1991)
- 6.31 J. Althoff: Properties and uses of a new heat-resistant Al–Mn alloy, *Metall* **31**, 263–267 (1977), in German
- 6.32 J. Althoff: Examples of the application-orientated development of high-strength aluminium manganese alloys, *Aluminium Engl. Suppl.* **56**, E37–E39 (1982), English translation
- 6.33 P. Brenner, H. Kostron: Treatment of AlMgSi-alloys, *Z. Metallkunde* **31**, 89–97 (1939)
- 6.34 I. Novikov: *Theory of Heat Treatment of Metals*, 1st edn. (Metalurgija, Moscow 1978)
- 6.35 Y. Takeuchi: Effect of plastic deformation on the natural ageing of AlCuMg1, AlCuMg2 and AlZnMgCu0.5, *Aluminium* **47**, 665–670 (1971), in German
- 6.36 K. Lücke, P. Stüwe: On the theory of impurity controlled grain boundary motion, *Acta Met.* **19**, 1067–1099 (1971)
- 6.37 H. Warlimont: Effect of segregation and precipitation on the recrystallisation and grain size of non-ferrous metals, *Freib. Forschungsh. B* **200**, 31–57 (1979), in German
- 6.38 E. Nes, S. Slevolden: Casting and annealing structures in strip cast alloy, *Aluminium* **55**, 319–324 (1979)
- 6.39 D.B. Goel, P. Furrer, H. Warlimont: Precipitation behaviour of AlMnCuFe-alloys, *Aluminium* **50**, 511–516 (1974), in German
- 6.40 C. Kammer, M. Krumnacker: Thermomechanical treatment of strip cast AlMn1Fe1 alloy, *Metall* **43**, 1162–1168 (1993), in German
- 6.41 E. Nes, J.D. Embury: The influence of a fine particle dispersion on the recrystallisation behaviour of a two phase aluminium alloy, *Z. Metall.* **66**, 589–593 (1975)
- 6.42 E. Nes, S. Slevolden: The concept of a grain size diagram in the analysis of the recrystallisation behaviour of AlMn-alloys, *Aluminium* **52**, 560–563 (1976)
- 6.43 E. Nes: The effect of a fine particle dispersion on heterogeneous recrystallisation, *Acta Met.* **24**, 391–398 (1976)
- 6.44 W. Huppertz: The fundamentals of corrosion protection of aluminium alloys used as structural materials. Part 1, *Metall* **49**, 505–509 (1995), in German